This is a preprint draft. The published article can be found at: https://doi.org/10.1016/j.istruc.2023.07.040.

Please cite this paper as:
Ghasemi A., Naser M.Z., (2023). "Tailoring 3D printed concrete through explainable artificial intelligence." *Structures*. https://doi.org/10.1016/j.istruc.2023.07.040.

Tailoring the Properties of 3D Printed Concrete through Explainable Artificial Intelligence

Alireza Ghasemi[1], M.Z. Naser[1,2]
[1]School of Civil and Environmental Engineering & Earth Science (SCEEES), Clemson University, Clemson, SC 29634, USA, E-mail: ghasemi.alireza2121@gmail.com,
[2]AI Research Institute for Science and Engineering (AIRISE), Clemson University, Clemson, SC 29634, USA
E-mail: mznaser@clemson.edu, Website: www.mznaser.com

Abstract

Advances on the construction front continue to rise as the next industrial revolution (Construction 4.0) nears. One promising front revolves around additively fabricated or simply 3D printed concrete. The growing number of ongoing parallel research programs has now made it possible to collect a large amount of data on such concrete as, up to this point, the open literature lacks a comprehensive database. Thus, this paper presents the largest database spanning over 300 experiments on 3D printed concrete. This database is then examined via multilinear regression as well as two explainable artificial intelligence (XAI) algorithms, namely, Random Forest and XGBoost, to arrive at a working model capable of predicting the compressive strength property for 3D concrete mixtures that incorporate the following seven features: age of specimens, as well as the magnitude of cement, water, fly ash, silica fume, fine aggregate, and superplasticizer. Findings from this work infer the superiority of XAI models in predicting the strength property of 3D printed concrete. Our analysis identifies two features, namely, the age of specimens and the quantity of fine aggregate, as the most important features that can accurately predict the compressive strength property. Finally, the deployed explainability methods successfully quantified the highly nonlinear relations between the selected features and compressive strength, and this newly acquired knowledge can help tailor functional concrete mixtures.

Keywords: 3D concrete; Compressive strength; Machine learning; Database.

1. Introduction

Traditionally, fabricating concrete relies on manually mixing and casting concrete via labor and formworks. This process requires extensive resources and often yields a large quantity of waste [1]. Recent works have identified such a negative impact and noted the continued loss of efficiency in construction [2]. The same works have also identified 3D printing of concrete as a noteworthy technology that has the potential to improve the current rates of construction productivity as well as minimize concrete wastage. It goes without saying that automating the process of construction brings a plethora of advantages, such as faster and safer construction [3]. According to a recent analysis by Markets and Markets [4], 3D printing concrete can save on construction waste by 30 to 60%, reduce labor costs by 50 to 80%, and fasten production time by 50 to 70%.

3D printing of concrete started to prosper in the mid-1990s [5]. This technology builds in a layer-after-layer approach using a 3D printer (casting equipment) [6,7]. In this printer, the raws are mixed and then injected via a nozzle [8]. To maintain a proper flow, the concrete mixture is designed to have acceptable pumpability and cohesiveness (to ensure strong buildability [9–11]). A number of large scale structures have been constructed from 3D printed concrete [12], including an apartment building [13] and a 26.3 m long bridge [14]. Figure 1 shows the latest state of 3D printed concrete in different countries around the world. This figure shows that the US, China, UK, and Germany have the most impact on 3D printed concrete and projects related to this material.

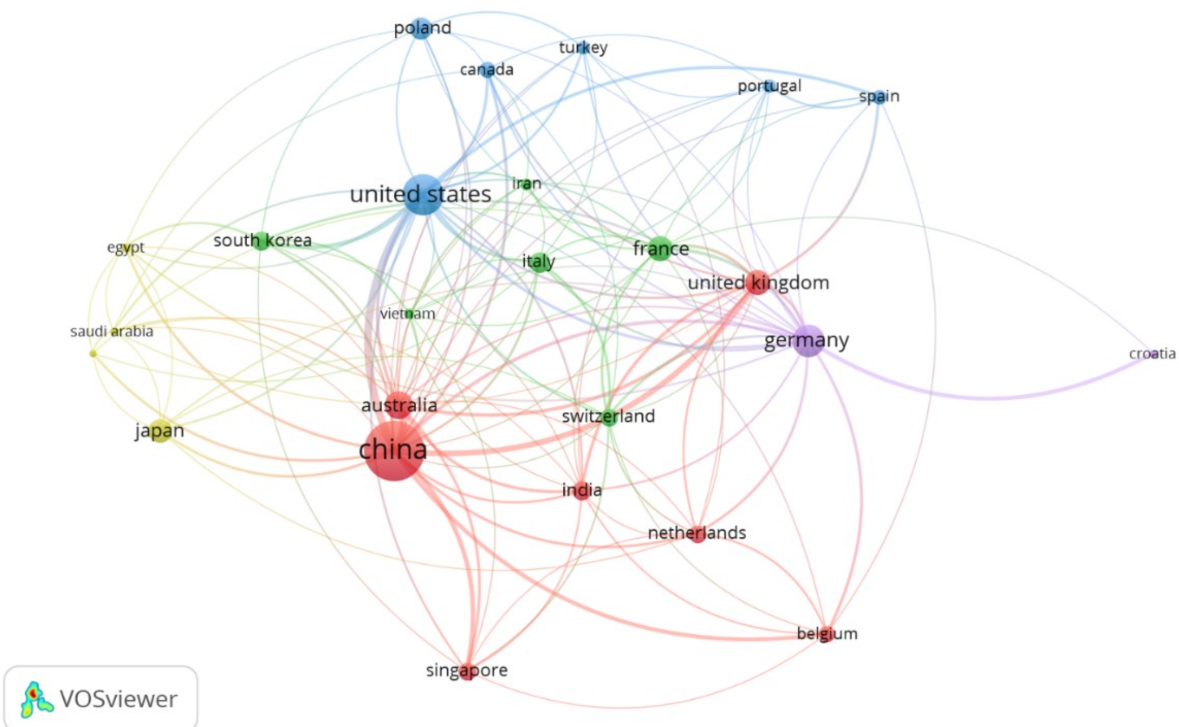

Fig. 1. Participation of countries in 3D printing concrete

Now, with a series of proof of concepts being constructed and validated, efforts have been targeting the creation of suitable material models to tailor 3D concrete mixtures. For example, the mechanical strength of concrete (i.e., compressive strength) is tied to other properties (modulus, tensile and flexural strength) and is a fixture in the codal provisions [15]. Thus, arriving at a reliable material model that can predict the compressive strength of 3D printed concrete as a function of mixture proportions would effective mixture designs and minimize reliance on "trial batching" approaches [16].

These traditional design techniques are based on trial-and-error methods emanating from experimental data [17]. However, the search space of such techniques exponentially grows for complex phenomena of complicated nonlinear relationships and non-quantitative materials [18]. To overcome the complexity of such nonlinear relations, researchers started to favor nonparametric models such as those created by machine learning (ML) [19]. Evidently, such predictive models have been developed for various concrete derivates – with little, if any, on 3D printed concrete [20]. As such, a key motivation behind this work is to create such ML models for 3D concrete.

This is a preprint draft. The published article can be found at: https://doi.org/10.1016/j.istruc.2023.07.040.

Please cite this paper as:
Ghasemi A., Naser M.Z., (2023). "Tailoring 3D printed concrete through explainable artificial intelligence." *Structures*. https://doi.org/10.1016/j.istruc.2023.07.040.

In general, ML models are primarily data-driven, and hence they rely on the availability of dense and healthy databases to uncover and map the relationships between the features involved and the compressive strength of 3D printed concrete [21]. Figure 2a displays the body of works related to ML in this area, and Fig. 2b shows the corresponding number of publications. The latter shows considerable growth from 120 publications in 2013 to approximately 2250 publications in 2022. Thus, machine learning (ML) can be selected as one of the hot topics in engineering.

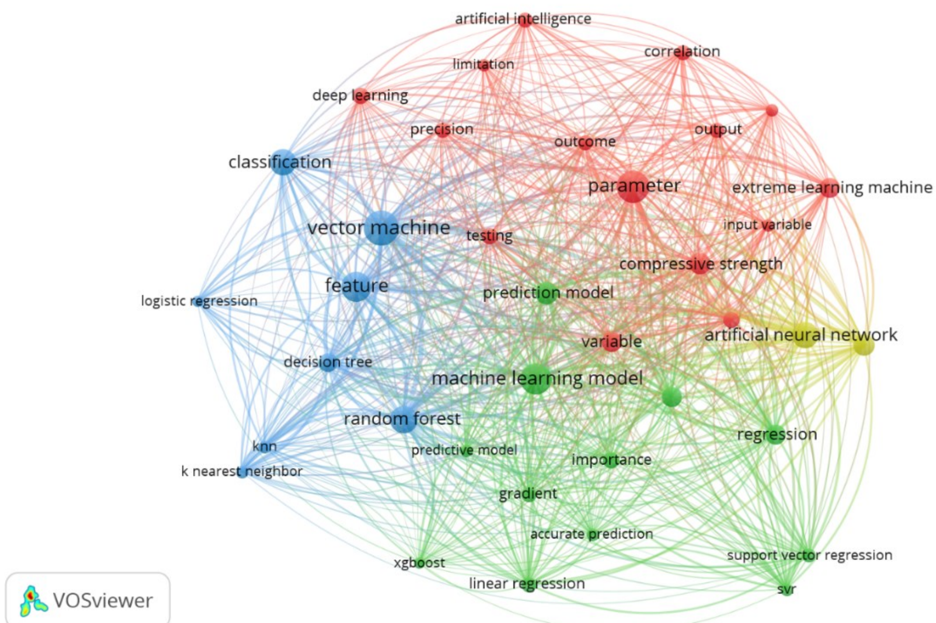

(a) Machine learning keywords in concrete

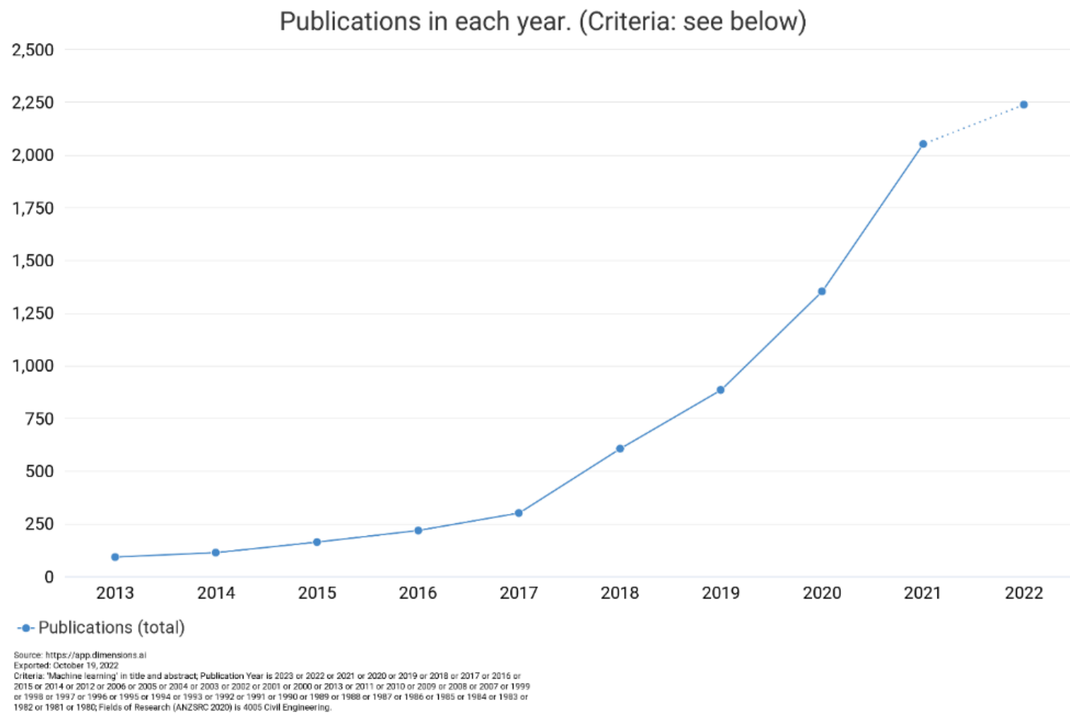

(b) Publication trends

Fig. 2. Current state of the art

A closer look into the reviewed publications reveals that ML has been used to predict the compressive strength of conventional concrete via artificial neural networks (ANN) [22], support vector machines (SVM) [23], decision trees [24–26], to name a few. For example, Lee [27] noted the high accuracy of ANN in predicting the properties of concrete mixtures. Further, Yeh et al. [28] used the Genetic Operation Tree (GOT) algorithm to predict the compressive strength of high performance concrete with great success. Nunez [29] concluded that ML had been verified to predict various concretes' compressive strengths. Han [30] reported that ANN and the random forest algorithm have high predictivity, especially in small datasets. Ozcan et al. [31] and Roa [32] reported similar success in predicting the compressive strength of concrete.

The aim of this study, and hope behind its investigation, is to (1) compile the largest database on the compressive strength of 3D printed concrete and to create explainable AI models to (2) predict the compressive strength of such concrete via XAI model. Thus, we will present results from 307 tests gathered from 53 different publications. In this database, seven features were collected (i.e., cement, silica fume, superplasticizer, water, fine aggregate, age, and fly ash) to predict the compressive strength. Then, this database was examined via multilinear regression as well as two explainable artificial intelligence (XAI) algorithms, namely, Random Forest and XGBoost, to arrive at material models. The results from our analysis show the superiority of the XAI models, and hence these models were augmented with explainability measures, namely, feature importance, accumulated local effects (ALE), and partial dependence plot (PDP), to quantify the highly nonlinear relations between features and compressive strength and hence may accelerate our research efforts.

This is a preprint draft. The published article can be found at: https://doi.org/10.1016/j.istruc.2023.07.040.

Please cite this paper as:
Ghasemi A., Naser M.Z., (2023). "Tailoring 3D printed concrete through explainable artificial intelligence." *Structures*. https://doi.org/10.1016/j.istruc.2023.07.040.

2. A brief overview of 3D printing of concrete

2.1 Past and current efforts

Khoshnevis pioneered 3D printing of concrete using the contour crafting method at the University of Southern California. Since then, much research and investments have been implemented to improve the performance of this innovative manufacturing method in many aspects, including extrudability, time setting, binder jetting, etc. [33]. Many universities and institutions have serious investments in experimental and numerical research (see Fig. 3a). Similarly, Fig. 3b shows a steady rise in the number of publications in this area as well.

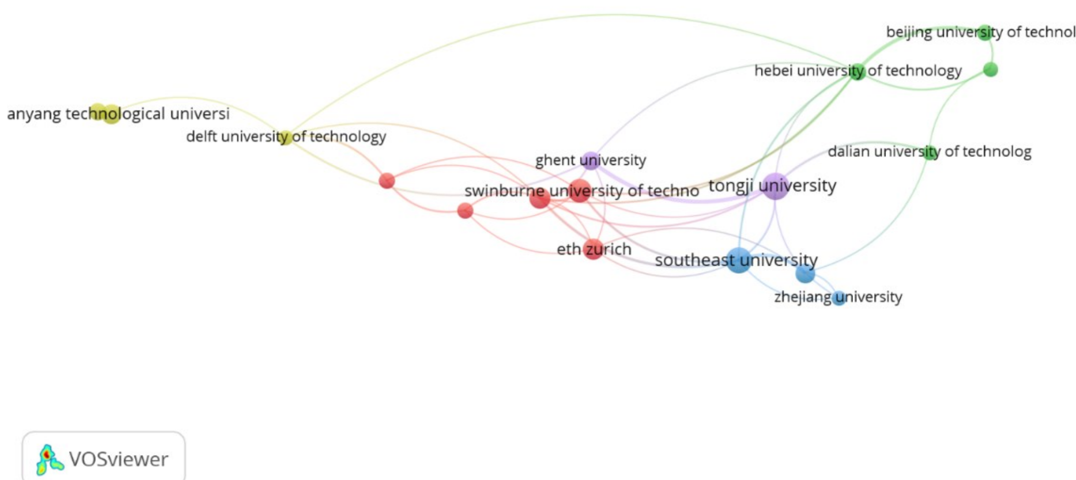

(a) Demonstration of universities active in 3D concrete

Please cite this paper as:
Ghasemi A., Naser M.Z., (2023). "Tailoring 3D printed concrete through explainable artificial intelligence." *Structures*. https://doi.org/10.1016/j.istruc.2023.07.040.

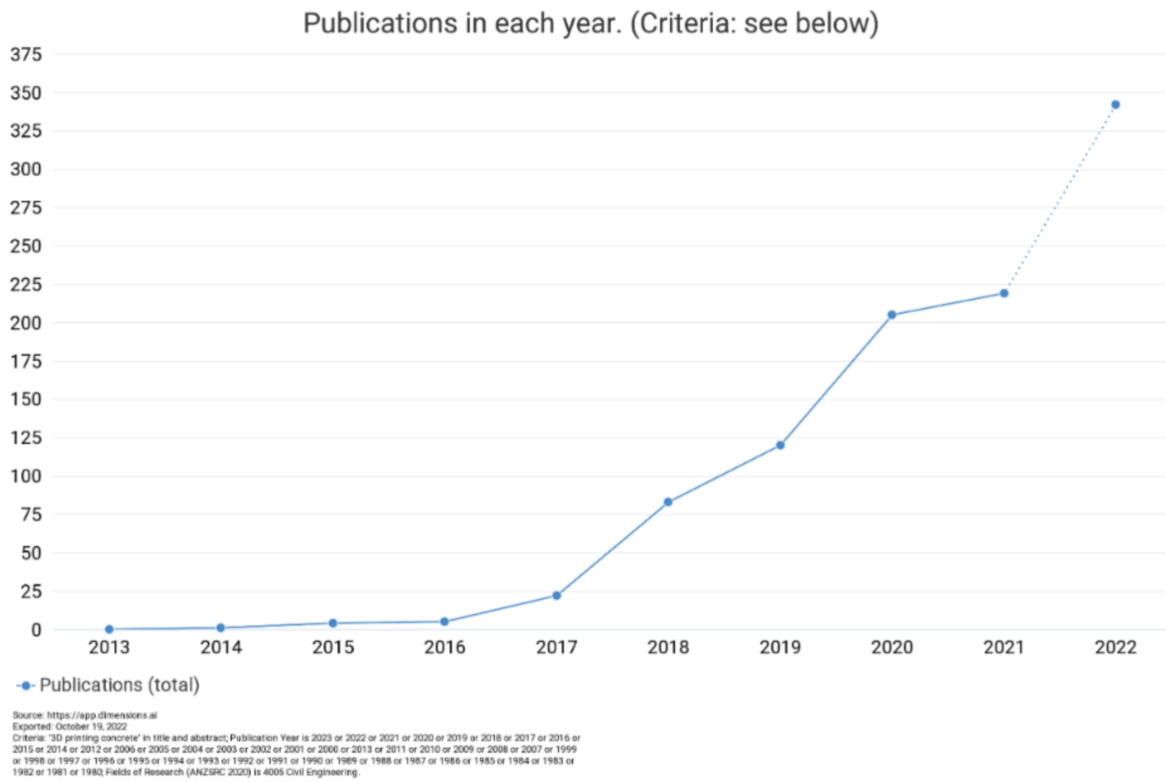

(b) Number of publications for 3D printing concrete [Note: as noted in the Dimension.ai database]

Fig. 3 Current state of the art

2.2 Trending areas of research

Proper grading of concrete leads to realizing stable structures [34,35][36]. There are four key areas that dominate the interest in the front of 3D concrete (see Fig. 3), namely;

1. *Extrudability* of cementitious material in a continuous manner is influenced by the size of dry materials such as fine aggregate [37][46] [39].
2. *Buildability* is defined as the ability of cementitious material to remain in a stable shape under loading [40–42].
3. *Open time* is often defined as the duration of time in which the cementitious material can maintain its performance through printing [43,44].
4. *Flowability* identifies the transportability of the cementitious materials, including fibers , during casting to the nozzle and can be evaluated via the slump test [45], the V-funnel test [46], and the jumping table test [47] [48].

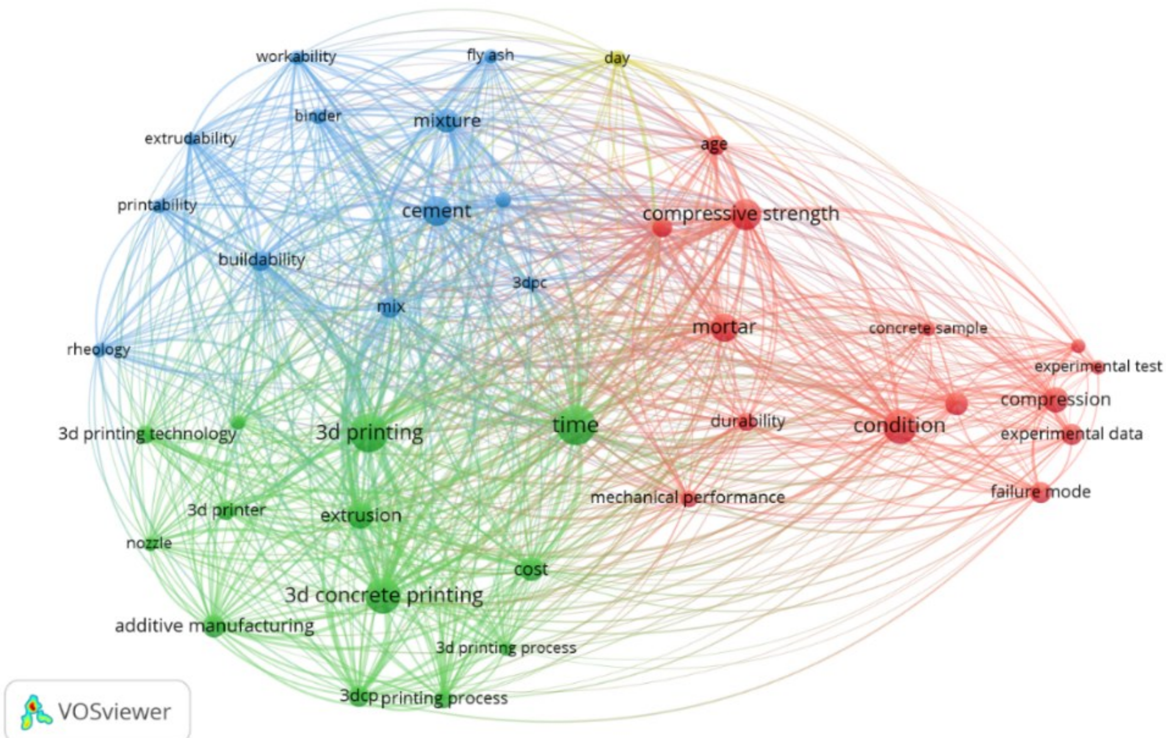

Fig. 3 The illustration of the body of works related to 3D printing concrete [from *Dimensions.ai* [49]]

2.3 Notable projects

As mentioned earlier, there is a continued rise and interest in adopting 3D printed concrete in construction projects [50–53]. For example, recent works explored reinforcing 3D printed concrete via fibers [54–56], traditional rebars and post-installed reinforcement, and mesh molds [57] Figure 4 shows some of the most notable and recent projects, including the building of the largest 3D printed pedestrian bridge in China in 2019 [58], retaining walls for flood mitigation in China in 2019 [59], residual buildings in Texas for the homeless in 2019 [60], apartments in Bavaria in 2021 [61], shelters for troops in 2021 in California [52], and the world's largest 3D printed structure in 2021 in UAE [50]. Another future goal is to fabricate extraterrestrial habitats [62].

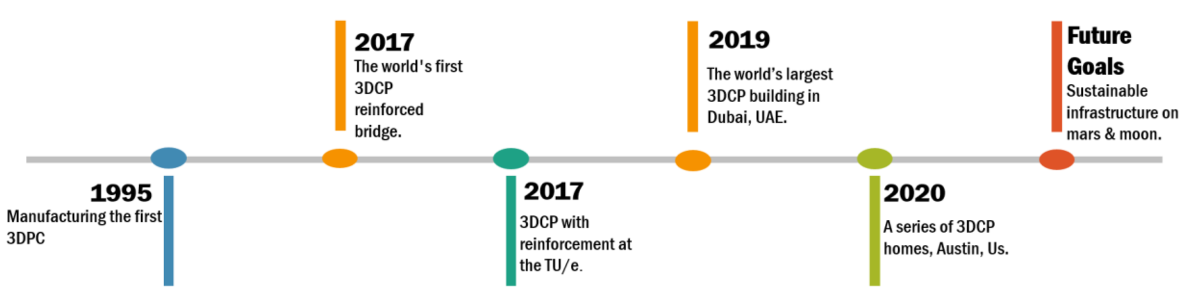

Fig. 4 Timeline for 3D concrete [Note: 3DPC denotes 3D printed concrete]

This is a preprint draft. The published article can be found at: https://doi.org/10.1016/j.istruc.2023.07.040.

Please cite this paper as:
Ghasemi A., Naser M.Z., (2023). "Tailoring 3D printed concrete through explainable artificial intelligence." *Structures*. https://doi.org/10.1016/j.istruc.2023.07.040.

3. Description of database and statistical analysis

The collected database for the present work has been compiled from 53 experimental studies and contains 307 specimens. This database has seven features, namely, cement (*C*), water (*W*), superplasticizer (*SP*), fly ash (*Fa*), silica fume (*SF*), fine aggregate (*FA*), age (*A*), and the response as compressive strength (CS) of each tested specimen. The seven features were selected as noted to be the most common factors and predictors in other types of concrete, such as high performance concrete [63,64], self-compacting concrete [65] and normal concrete [66]. Please note that all data used in this study will be provided in this paper's appendix.

The statistical distribution of this database is shown in Fig. 5. Similarly, Table 1 describes the overview of the statistics of the data. These statistics show that the overall range of components in our dataset is normal and acceptable, as commonly witnessed in recent tests. The same table shows that cement, water, and fine aggregate are fairly symmetrical (skewness is between -0.5 and 0.5), while age and compressive strength are moderately skewed (skewness -1 and -0.5 or between 0.5 and 1). Finally, fly ash, silica fume, and superplasticizer are noted to be highly skewed since these components were used at various values in different experiments and were not used at all in others.

Table 1 Statistical insights into the features

Component	Minimum	Maximum	Mean	Standard Deviation	Skew	Kurtosis
Cement, C (Kg/m^3)	0	1069.41	502.18	228.88	0.37	-0.12
Water, W (Kg/m^3)	1.89	455	213.07	98.47	0.41	0.29
Fly ash, Fa (Kg/m^3)	0	1026	113.16	162.51	2.77	11.1
Silica fume, SF (Kg/m^3)	0	345	43.25	57.24	2.46	8.93
Fine aggregate, FA (Kg/m^3)	0	1623	797.83	449.89	-0.27	-1.19
Superplasticizer, SP (%)	0	3.4	1.44	3.63	6.96	57.7
Age, (day)	0.41	56	15.73	12.74	0.51	-0.33
Compressive strength, CS (MPa)	0.005	125	40.82	23.01	0.77	0.79

This is a preprint draft. The published article can be found at: https://doi.org/10.1016/j.istruc.2023.07.040.

Please cite this paper as:
Ghasemi A., Naser M.Z., (2023). "Tailoring 3D printed concrete through explainable artificial intelligence." *Structures*. https://doi.org/10.1016/j.istruc.2023.07.040.

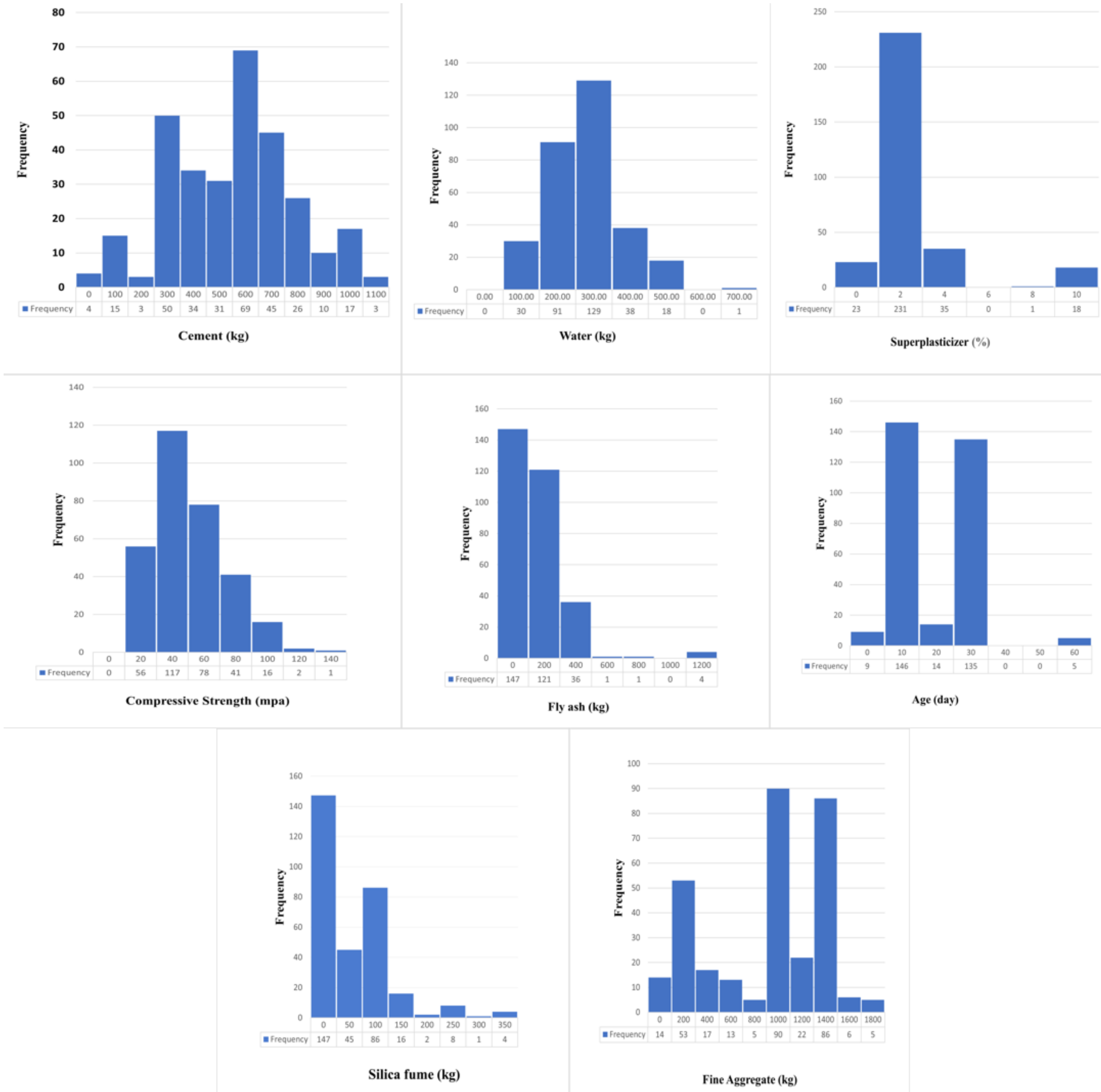

Fig. 5. The frequency of features

In addition, Fig. 6a, describes the Pearson correlation matrix for the database. This matrix displays the linear relation between feature pairs to be between -1 and +1 (approaching unity implies a strong linear correlation). This matrix shows that the linear correlation between age and compressive strength is the highest and is at 0.48. Collectively, there is not a large linear correlation within the database. For instance, the Pearson correlations between cement and silica fume with compressive strength are 0.096 and 0.14, respectively.

It should be noted that there is a low correlation between water and superplasticizer and strength. In lieu of the Pearson correlation, the Spearman correlation matrix displays the monotonic relation within the database (see Fig. 6b). Like the Pearson correlation, the range of correlations is also between -1 and +1. From this view, the features of noteworthy monotonic relation are the age (0.49), followed by a weaker association in silica fume (0.25) and cement (0.13).

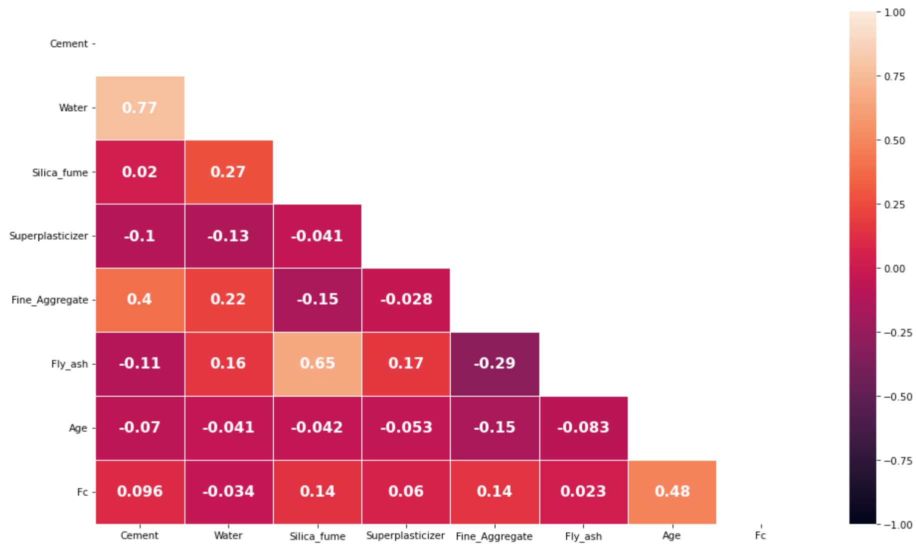

(a) Pearson correlation matrix

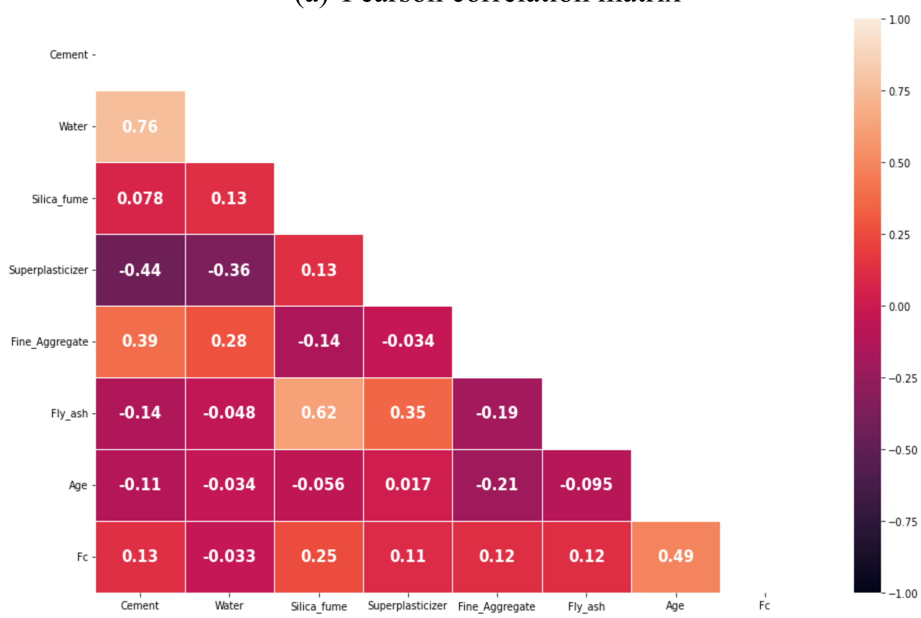

This is a preprint draft. The published article can be found at: https://doi.org/10.1016/j.istruc.2023.07.040.

Please cite this paper as:
Ghasemi A., Naser M.Z., (2023). "Tailoring 3D printed concrete through explainable artificial intelligence." *Structures*. https://doi.org/10.1016/j.istruc.2023.07.040.

(b) Spearman correlation matrix

Fig. 6 Pearson and Spearman matrices

This is a preprint draft. The published article can be found at: https://doi.org/10.1016/j.istruc.2023.07.040.

Please cite this paper as:
Ghasemi A., Naser M.Z., (2023). “Tailoring 3D printed concrete through explainable artificial intelligence.” *Structures*. https://doi.org/10.1016/j.istruc.2023.07.040.

4. Machine learning algorithms

The compiled database was examined through three algorithms: multilinear regression, XGBoost, and Random Forest. We carried out the machine learning analysis by using the Python Scikit-learn [67] package. These are briefly described herein. Please note that all codes used in this study will be provided in the appendix of this paper.

4.1 Multilinear regression

In general, linear regression can be categorized into two classes: simple-linear regression and multilinear regression [68]. The latter is of interest to this work as multilinear regression considers the effects of multiple features (x) to predict a target (y) [69][70]. The formula of multilinear regression is presented in Eq. 1.

$$y = b_0 + b_1 x_1 + b_2 x_2 + \cdots + b_i x_i \tag{1}$$

Where $b_1, b_2, \ldots, b_i$ are the weights and b_0 is the y-intercept. Please note that the error is not shown in this equation.

4.2 XGBoost

The XGBoost is a tree-based algorithm that adopts ensemble learning (i.e., combining individual models) [71]. This algorithm prevents overfitting with the regularized boosting method and can automatically handle missing values. Moreover, the XGBoost can cross-validate at each iteration. After each iteration, the algorithm’s learning rate is adjusted as a weight on each training (i. e. Eta Hyperparameter) [72].

4.3 Random Forest

The random forest algorithm is a collection of decision trees [73]. Each decision tree splits the input data recursively using the decision nodes, and the optimal split is found by increasing the entropy gain. This algorithm takes the average value of all decision trees to arrive at the final outcome [74][75].

4.4 Details on ML analysis

In this analysis, the database was split into two datasets, namely, the training dataset and the testing dataset. In our model, 80% of the total dataset (261 samples) was selected as training, and remained dataset (66 samples) was considered as test-size. This split ratio was arrived at via sensitivity analysis and is commonly used in concrete problems, as noted in a recent review [76]. Before fitting the data in our model, the dataset was normalized since there were seven different features with seven different units and magnitudes. By normalization, the values of numeric features in our dataset were altered to a common scale without distorting differences in the ranges of values or losing information.

4.4.1 k-cross validation method

The *k*-cross validation method is used herein to develop all ML models [77]. In a *k*-fold cross validation, a dataset is divided into *k* datasets with the same numbers. In each validation process, one dataset is selected for testing the model, and remained datasets are considered for training the model – see Fig. 7 [78].

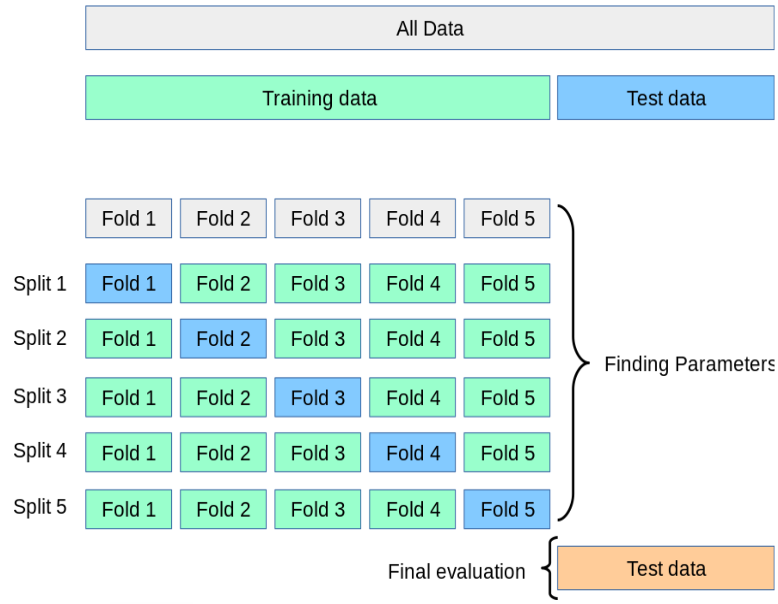

Fig. 7 Schematic of *K*-Cross Validation [79]

4.4.2 Performance Evaluation

Four commonly used metrics in the area of concrete were selected, namely, Mean Absolute Error (MAE), Mean Squared Error (MSE), root-mean-square deviation (RMSE), and coefficient of determination (R^2) in order to evaluate the accuracy of the ML models [80].

Mean squared error (MSE)

The mean squared error (MSE) is another metric that can evaluate the performance of a model. As it is calculated based on the square of Euclidean distance, it is always a positive number that decreases as the error approaches zero. Thus, it can be one of the preferred metrics for loss functions since it exaggerates the errors (i.e., squared distances between anticipated and actual values).

$$\mathrm{MSE} = \frac{1}{n}\sum_{i=1}^{n}(y_i - \hat{y}_i)^2 \tag{2}$$

Coefficient of determination (R^2)

The *coefficient of determination* is called R^2 and yields a value between -1 and +1. This metric measures the proportion of the variance of a dependent variable that is explained by a regression model and defined by:

$$R^2 = 1 - \frac{\sum_{i=1}^{n}(y_i - \hat{y}_i)^2}{\sum_{i=1}^{n}(y_i - \bar{y})^2} \tag{3}$$

Where y_i is an observed target, $\hat{y_i}$ is the predicted target of the regression model, both indexed by i, and $\bar{y}$ is the mean of the dependent variable.

This is a preprint draft. The published article can be found at: https://doi.org/10.1016/j.istruc.2023.07.040.

Please cite this paper as:
Ghasemi A., Naser M.Z., (2023). "Tailoring 3D printed concrete through explainable artificial intelligence." *Structures*. https://doi.org/10.1016/j.istruc.2023.07.040.

Mean absolute error (MAE)

The mean absolute error (MAE) calculates the error based on *variances* between predictions and the ground truth. This metric is computed as the total sum of errors divided by the number of experiments in order to take an average of errors.

$$\mathrm{MAE} = \frac{\sum_{i=1}^{n}|y_i - x_i|}{n} \tag{4}$$

Root mean square error (RMSE)

The root Mean Square Error (RMSE) is the standard deviation of the residuals (i.e., prediction error) and can be calculated as shown.

$$RMSE = \sqrt{\frac{\sum_{i=1}^{n}(y_i - \hat{y}_i)^2}{n}} \tag{5}$$

5. Discussion and results

This section details the outcome of our analysis. As mentioned above, all models were assessed by four different metrics, namely, mean squared error (MSE), coefficient of discrimination (R^2), root mean squared error (RMSE), and mean absolute error (MAE).

5.1 Multilinear regression

Equation 6 presents the outcome of the multilinear regression analysis. Given the largest magnitude of their weights, this equation reveals that age and superplasticizers have the largest influence on the model. Table 2 further shows the performance of this model. As can be seen, this model did not perform adequately and scored poorly, especially with regard to R^2 as well as in relation to the observed residuals (see Fig. 8). By looking at Fig. 8; one can reinforce the notion that the performance of this particular model is indeed poor. This can be an indication of the assumption that linearity between the features and strength is faulty.

$$y = 13.18 - 0.085x_1 + 0.032x_2 + 0.984x_3 + 0.0776x_4 + 0.010x_5 + 0.006x_6 + 0.567x_7 \tag{6}$$

Where $x_1, x_2, x_3, x_4, x_5, x_6$ *and* x_7 are coefficients for water, cement, age, silica fume, fine aggregate, fly ash, and superplasticizer, respectively.

Table 2 Performance of the multilinear regression model

Metrics	Training dataset	Testing dataset
MSE	288.77	405.63
R^2	0.233	0.422
MAE	13.31	16.14
RMSE	16.99	20.14

This is a preprint draft. The published article can be found at: https://doi.org/10.1016/j.istruc.2023.07.040.

Please cite this paper as:
Ghasemi A., Naser M.Z., (2023). "Tailoring 3D printed concrete through explainable artificial intelligence." *Structures*. https://doi.org/10.1016/j.istruc.2023.07.040.

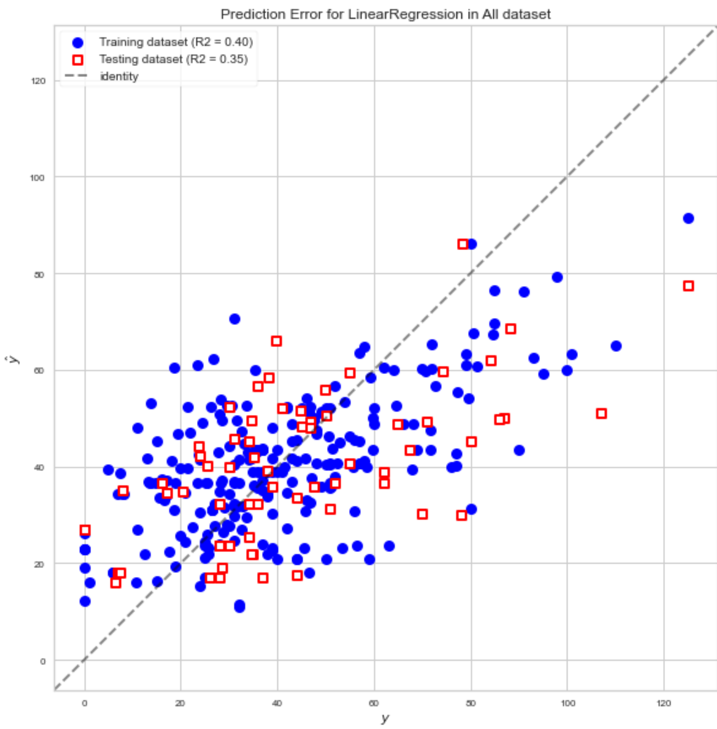

Fig. 8 Comparison of model performance

5.2 XGBoost

The metrics for the XGBoost model are listed in Table 3. As noted here, this model substantially outperforms the multilinear model. For instance, the coefficient of discrimination (R^2) experienced a sharp increase from 0.233 in multilinear regression to 0.981 in XGBoost in training and from 0.422 to 0.831 in testing. A similar observation can be seen in Fig. 9.

Table 3 Performance of model

Metrics	Training dataset	Testing dataset
MSE	7.30	213.33
R^2	0.981	0.831
MAE	1.05	8.37
RMSE	2.71	14.60

This is a preprint draft. The published article can be found at: https://doi.org/10.1016/j.istruc.2023.07.040.

Please cite this paper as:
Ghasemi A., Naser M.Z., (2023). "Tailoring 3D printed concrete through explainable artificial intelligence." *Structures*. https://doi.org/10.1016/j.istruc.2023.07.040.

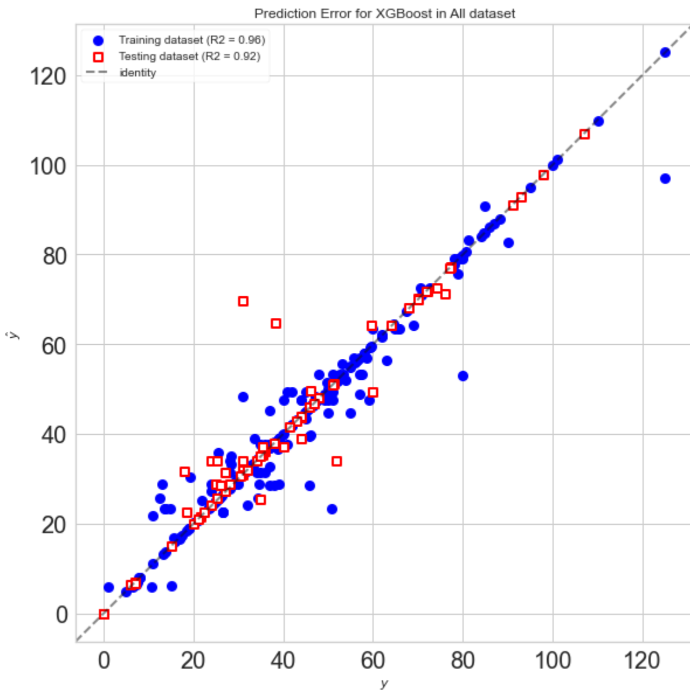

Fig. 9 Comparison of model performance

5.3 Random forest regression metric

Table 4 lists the result of the random forest model on two different datasets (i.e., the training dataset and the testing dataset). As one can see, this model performs well across the training and testing datasets. In addition, the results of this analysis also show that this model outperforms all other models examined herein. Figure 10 also confirms this observation.

Table 4 Performance of model

Metrics	Training dataset	Testing dataset
MSE	23.72	75.60
R^2	0.956	0.846
MAE	3.30	6.00
RMSE	4.87	8.70

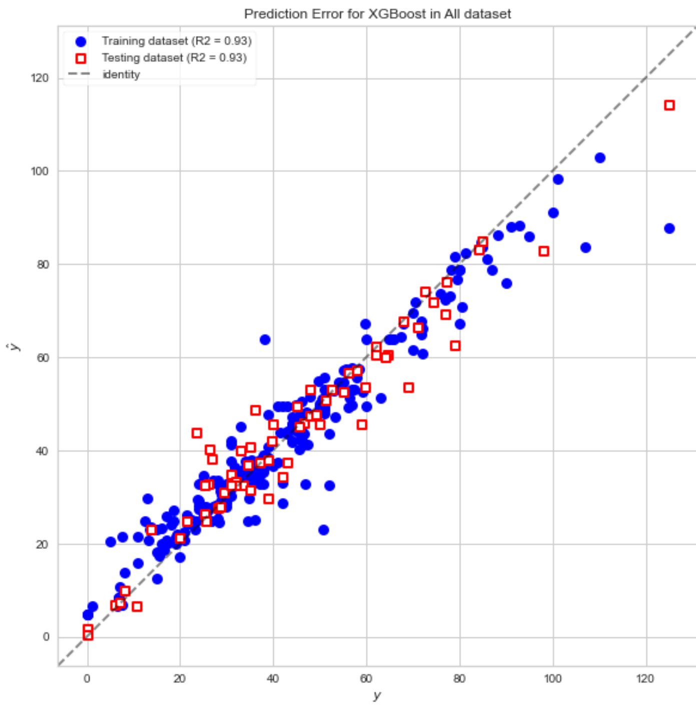

Fig. 10 Comparison of model performance

5.4. Explainability analysis

As mentioned above, the random forest is the best performing model in this study. Thus, we will apply explainability measures to this model to gain valuable insights into its performance and the influence of each of the features on the accurate predictions of compressive strength. Each explainability measure is explained and demonstrated herein.

5.4.1 SHAP summary and feature importance plots

The SHAP (SHaply Additive explanation) is a game theory-based method that allows users to peek into the reasoning of ML algorithms. When applied to a specific ML model, SHAP can generate a series of visualizations. Two such representations include the summary plot and the feature importance plot.

The summary plot describes each feature's importance by showing its range's influence on accurate predictions (see Fig. 11a). The summary plot's color illustrates each feature's value from low to high. Low values are associated with soft (blue) color, while bright (red) color defines high values. Each point in the summary plot represents one observation from the compiled database. The positivity and negativity of each point on model predictions can be observed in the horizontal axis of this plot. Positivity means the selected sample increases the prediction accuracy and vice versa.

Looking at Fig. 11 shows that age has the broadest distribution in comparison to other features and hence can significantly affect the predictions. On the other hand, fly ash is associated with the narrowest distribution, hence its small influence on model predictions. The same figure shows that the age, fine aggregate, and silica fume with high value (i, e. red color) positively impact the model's predictions of accurately capturing the compressive strength. In other words, the aforenoted features are identified to be the best features that have led to accurately predicting the compressive strength. On the contrary, a large quantity of water negatively affects the predictions, possibly as it affects the flowability and strength of concrete (which was also noted by [81,82]).

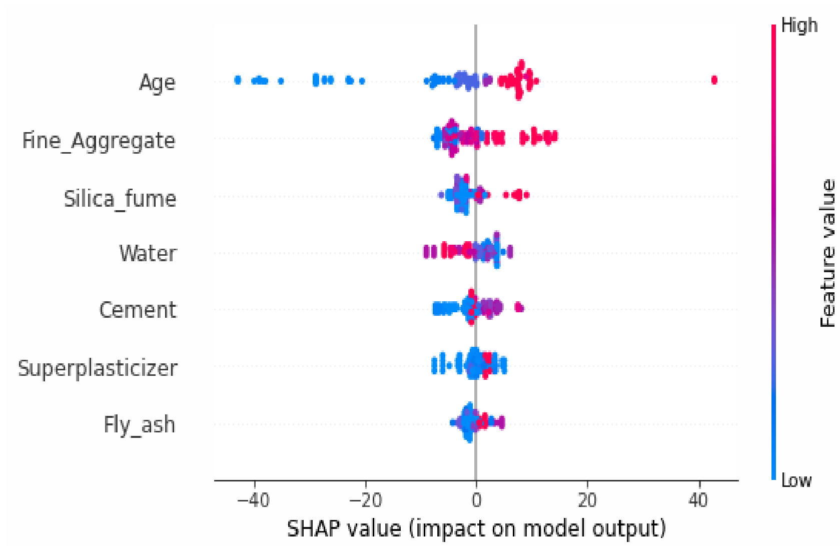

(a) Summary plot of SHAP values

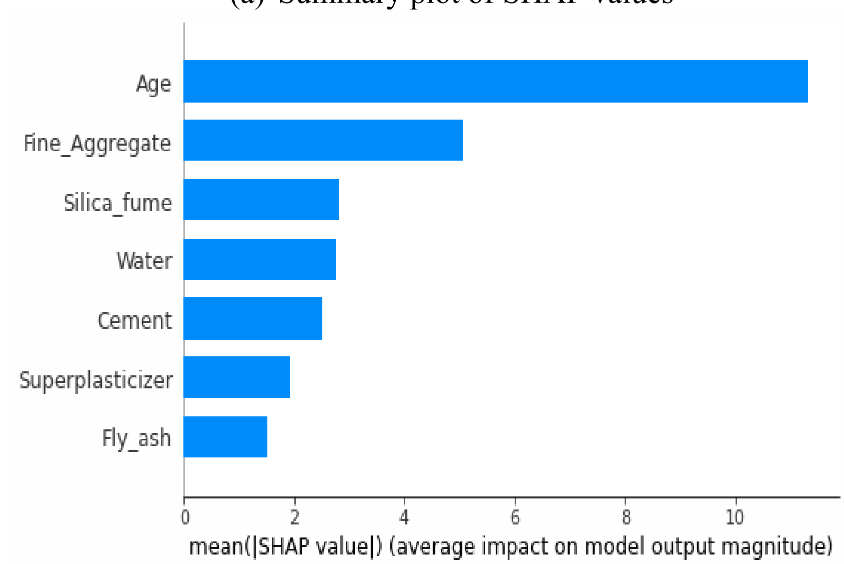

(b) Factor importance plot

Fig. 11 Results of SHAP analysis

Figure 11b builds on Fig. 11a and ranks the features in terms of their importance. As one can see, the summary plot of SHAP value does not articulate how each feature influences the model's prediction capability. For instance, this figure shows that age is the most influential feature but does not state if the influence is positive or negative. In other words, this particular figure indicates that the model heavily relied on age to arrive at accurate predictions of the compressive strength (as opposed to its reliance on fly ash or superplasticizers).

5.4.2 Partial dependence plots

The partial dependence plot (PDP) is the third explainability measure that will be employed herein. This plot explains the relation of each feature on predictions by plotting how varying the value of a feature while keeping all other features constant alter the final output of a model – see Fig. 12 [83]. Figure 12 shows that the strength increases with age – more so significantly after the first few days. Similarly, increasing the amount of cement also increases the compressive strength of 3D concrete. But, at around 700 kg of cement, the increase in strength seems to stabilize. On the other hand, the compressive strength is seen to fluctuate at some distinct proportions of some features. For example, the strength starts to drop slightly beyond 250 kg of water. This same is also seen in fly ash between 50 and 200 kg. For some features, namely, fly ash or superplasticizers, their values do not seem to affect model predictions by much.

5.4.3 Accumulated local effect (ALE)

It is worth noting that PDPs are designed to maintain the assumption of i**ndependence** of features, and hence these plots do not distinguish for correlation. Thus, to remedy this limitation, the accumulated local effects (ALE) plot is applied. The ALE plots are unbiased alternatives because they address the bias that arises in PDP when a feature is highly correlated with other features [84]. Comparing the vertical axis of PDPs and ALEs shows these axes differ. For example, this in a PDP represents the marginal impact of features on the response. In other words, it does not represent this variable's predicted value or relative impactn other variables [85]. On the other hand, the effect of each feature on the response, as given by the value of the feature, is presented in the vertical axis in ALEs.

Further, an ALE averages over the features using the conditional distribution $p(x_2|x_1)$ rather than the marginal distribution $p(x_2)$ as in PDP. This avoids extrapolating the data to unrealistic combinations of feature values, as in PDP. Instead of averaging model predictions, ALE averages over the change in model predictions, which represents the local effect of $x_1$on $f(x_1, x_2)$. This effectively blocks and offsets possible correlations that might exist between a feature x_1 and other features [86].

Figure 12 shows ALEs for all involved features. It is clear that there is a convergence between the PDPs and ALEs. For example, having a mixture be 20 and 50 days old is seen to increase the compressive strength by 10 and 20 MPa, on average, respectively.

5.4.4 Tailoring the strength of 3D concrete via XAI

The same figure can be used to tailor concrete mixtures for specific strengths. For example, to maximize the compressive strength, a mixture is expected to have the following proportions:

- Cement 600-700 kg. → leads to an increase of 4-7 MPa.
- Water: less than 100 kg. → leads to an increase of about 7.5 MPa.
- Fine aggregates > 1200 kg. → leads to an increase of about 0.5 MPa.
- Silica fume > 70 kg. → leads to an increase of about 12.5 MPa.

In a way, this figure can help designers tailor 3D mixtures for a given strength.

This is a preprint draft. The published article can be found at: https://doi.org/10.1016/j.istruc.2023.07.040.

Please cite this paper as:
Ghasemi A., Naser M.Z., (2023). "Tailoring 3D printed concrete through explainable artificial intelligence." *Structures*. https://doi.org/10.1016/j.istruc.2023.07.040.

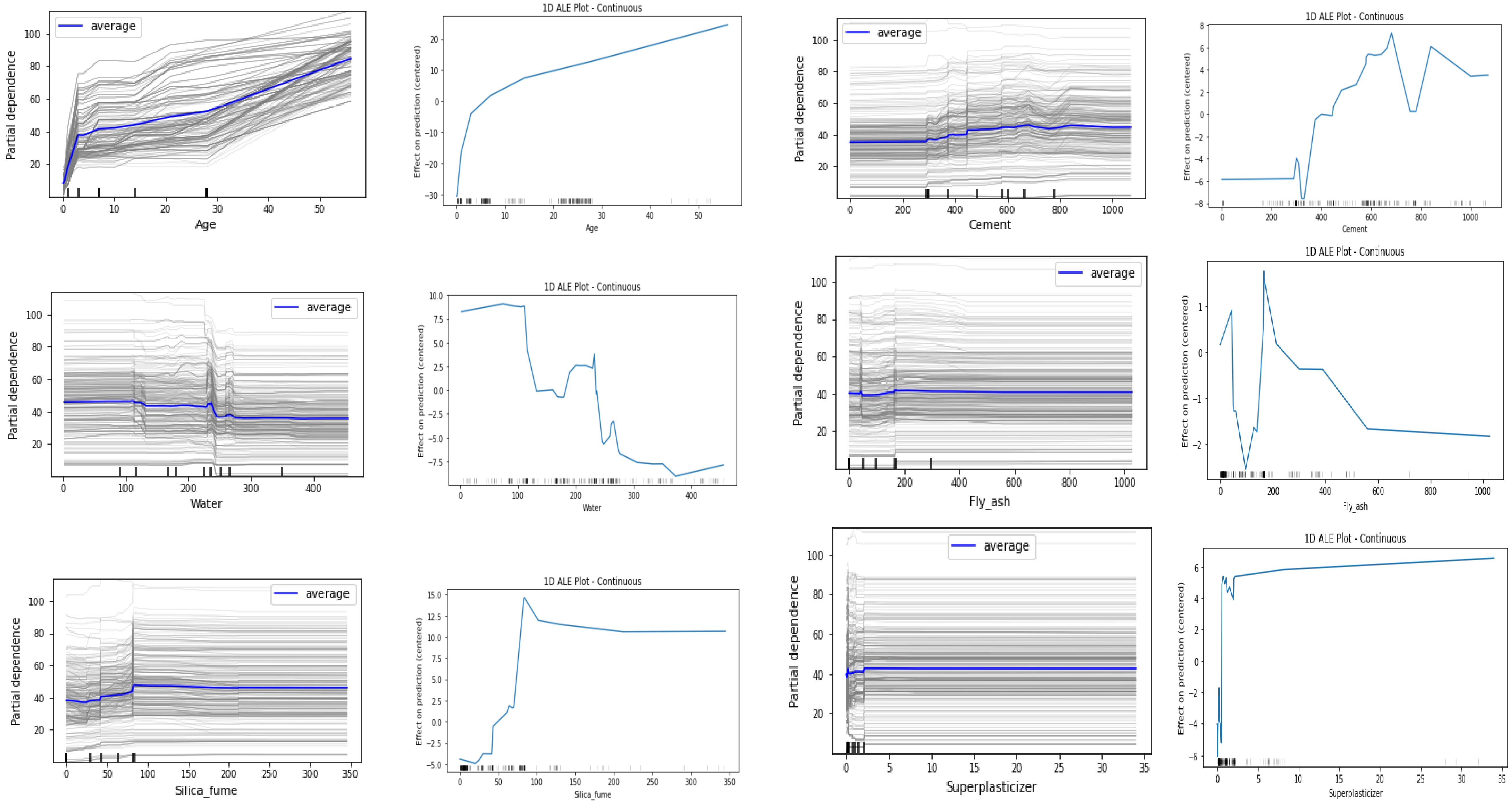

This is a preprint draft. The published article can be found at: https://doi.org/10.1016/j.istruc.2023.07.040.

Please cite this paper as:
Ghasemi A., Naser M.Z., (2023). "Tailoring 3D printed concrete through explainable artificial intelligence." *Structures*. https://doi.org/10.1016/j.istruc.2023.07.040.

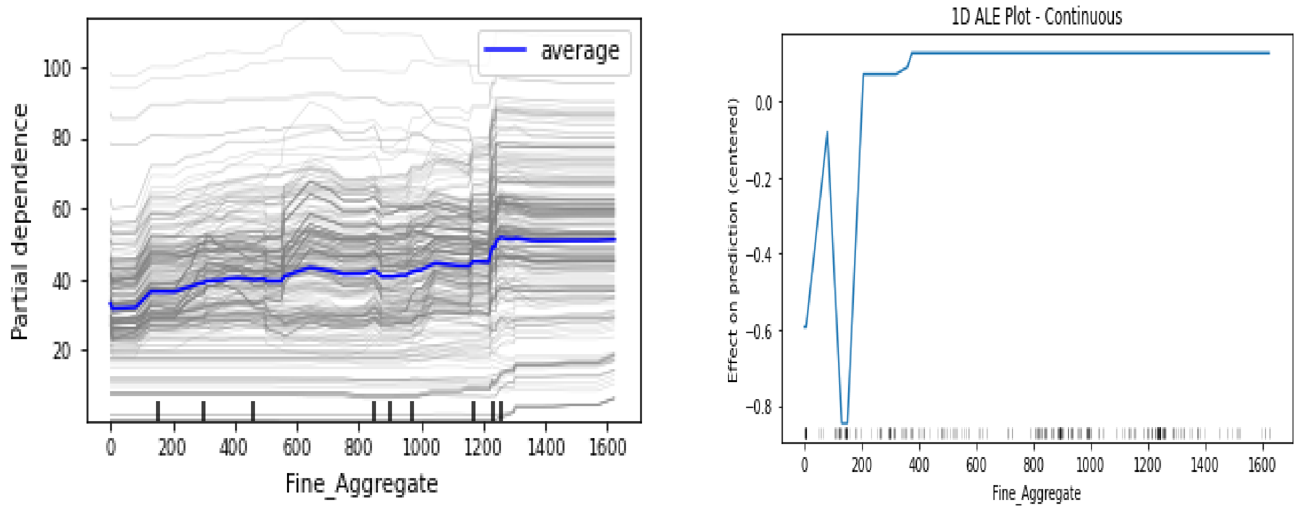

Fig. 12 Partial dependence plot (PDP) and accumulated local effects (ALE)

This is a preprint draft. The published article can be found at: https://doi.org/10.1016/j.istruc.2023.07.040.

Please cite this paper as:
Ghasemi A., Naser M.Z., (2023). "Tailoring 3D printed concrete through explainable artificial intelligence." *Structures*. https://doi.org/10.1016/j.istruc.2023.07.040.

6. Conclusions

This paper examines the predictability of 3D printed concrete through machine learning. Based on the 307 analyzed and compiled samples from previous literature and also seven feature variables, the compressive strength of 3D printing concrete has been anticipated and validated by 5-fold cross-validation with two repetitions. Three different algorithms, namely, random forest regressor, XGBoost regressor, and multilinear regression, are implemented in this study. In addition, the performance of our model was assessed by metrics, namely, R^2, MAE, MSE, and RMSE**.** For each algorithm, the prediction error plot and residual plot are included.

The main results are listed herein:

- The random forest model has reached an average 90.6% accuracy and thus performed the best compared to XGBoost.
- The age of 3D printing concrete is the most influential factor for predicting compressive strength, followed by the fine aggregate, cement, water, and silica fume. On the contrary, the superplasticizer and fly ash have the least effect on the target.
- XAI methods successfully quantified the highly nonlinear relations between features and compressive strength. This can allow us to tailor functional concrete mixtures.
- Future works should continue and extend this research. We encourage researchers to expand and collect more data on 3D concrete such that this research grows at a faster rate with the integration of XAI methods.
- To further amplify the positive use of AI in this area, we suggest exploring the use of physics-informed AI, together with XAI.

References

[1] S. Hou, Z. Duan, J. Xiao, J. Ye, A review of 3D printed concrete: Performance requirements, testing measurements and mix design, Constr Build Mater. 273 (2021) 121745. https://doi.org/10.1016/j.conbuildmat.2020.121745.

[2] S. Al-Qutaifi, A. Nazari, A. Bagheri, Mechanical properties of layered geopolymer structures applicable in concrete 3D-printing, Constr Build Mater. 176 (2018) 690–699. https://doi.org/10.1016/j.conbuildmat.2018.04.195.

[3] Kreiger, Megan A., Bruce A. MacAllister, Juliana M. Wilhoit, Michael P. Case, The current state of 3D printing for use in construction, In The Proceedings of the 2015 Conference on Autonomous and Robotic Construction of Infrastructure. (2015) 149–158.

[4] https://www.3printr.com/3d-concrete-printing-market-reach-56-4-million-2021- 123966/, (n.d.).

[5] F. Bos, R. Wolfs, Z. Ahmed, T. Salet, Additive manufacturing of concrete in construction: potentials and challenges of 3D concrete printing, Virtual Phys Prototyp. 11 (2016) 209–225. https://doi.org/10.1080/17452759.2016.1209867.

[6] A.V. Rahul, M. Santhanam, H. Meena, Z. Ghani, 3D printable concrete: Mixture design and test methods, Cem Concr Compos. 97 (2019) 13–23. https://doi.org/10.1016/j.cemconcomp.2018.12.014.

This is a preprint draft. The published article can be found at: https://doi.org/10.1016/j.istruc.2023.07.040.

Please cite this paper as:
Ghasemi A., Naser M.Z., (2023). "Tailoring 3D printed concrete through explainable artificial intelligence." *Structures*. https://doi.org/10.1016/j.istruc.2023.07.040.

[7] M. Papachristoforou, V. Mitsopoulos, M. Stefanidou, Evaluation of workability parameters in 3D printing concrete., Procedia Structural Integrity. (2018) 155–162.

[8] Y. Weng, B. Lu, M. Li, Z. Liu, M.J. Tan, S. Qian, Empirical models to predict rheological properties of fiber reinforced cementitious composites for 3D printing, Constr Build Mater. 189 (2018) 676–685. https://doi.org/10.1016/j.conbuildmat.2018.09.039.

[9] Y. Weng, M. Li, M.J. Tan, S. Qian, Design 3D printing cementitious materials via Fuller Thompson theory and Marson-Percy model, Constr Build Mater. 163 (2018) 600–610. https://doi.org/10.1016/j.conbuildmat.2017.12.112.

[10] Y.W.D. Tay, Y. Qian, M.J. Tan, Printability region for 3D concrete printing using slump and slump flow test, Compos B Eng. 174 (2019) 106968. https://doi.org/10.1016/j.compositesb.2019.106968.

[11] N. Roussel, Rheological requirements for printable concretes, Cem Concr Res. 112 (2018) 76–85. https://doi.org/10.1016/j.cemconres.2018.04.005.

[12] S. Hou, Z. Duan, J. Xiao, J. Ye, A review of 3D printed concrete: Performance requirements, testing measurements and mix design, Constr Build Mater. 273 (2021) 121745. https://doi.org/10.1016/j.conbuildmat.2020.121745.

[13] http://www.winsun3d.com. (accessed 18 October 2020) ARTIFICIAL NEURAL NETWORKS, (n.d.).

[14] J. Zhang, J. Wang, S. Dong, X. Yu, B. Han, A review of the current progress and application of 3D printed concrete, Compos Part A Appl Sci Manuf. 125 (2019) 105533. https://doi.org/10.1016/j.compositesa.2019.105533.

[15] A. Shishegaran, H. Varaee, T. Rabczuk, G. Shishegaran, High correlated variables creator machine: Prediction of the compressive strength of concrete, Comput Struct. 247 (2021) 106479. https://doi.org/10.1016/j.compstruc.2021.106479.

[16] B.A. Young, A. Hall, L. Pilon, P. Gupta, G. Sant, Can the compressive strength of concrete be estimated from knowledge of the mixture proportions?: New insights from statistical analysis and machine learning methods, Cem Concr Res. 115 (2019) 379–388. https://doi.org/10.1016/j.cemconres.2018.09.006.

[17] S.M. Gupta, Support vector machines based modelling of concrete strength, World Acad Sci Eng Technol. 36 (2007) 305–311.

[18] DeRousseau M.A., E. Laftchiev, Kasprzyk J.R., B. Rajagopalan, Srubar III WV, A comparison of machine learning methods for predicting the compressive strength of field-placed concrete, Constr Build Mater. 228 (2019) 116661.

[19] A. Behnood, V. Behnood, M. Modiri Gharehveran, K.E. Alyamac, Prediction of the compressive strength of normal and high-performance concretes using M5P model tree algorithm, Constr Build Mater. 142 (2017) 199–207.

[20] I.-C. Yeh, Modeling of strength of high-performance concrete using artificial neural networks, Cem Concr Res. 28 (1998) 1797–1808. https://doi.org/10.1016/S0008-8846(98)00165-3.

[21] J.-S. Chou, C.-F. Tsai, A.-D. Pham, Y.-H. Lu, Machine learning in concrete strength simulations: Multi-nation data analytics, Constr Build Mater. 73 (2014) 771–780. https://doi.org/10.1016/j.conbuildmat.2014.09.054.

[22] A. Öztaş, M. Pala, E. Özbay, E. Kanca, N. Çagˇlar, M.A. Bhatti, Predicting the compressive strength and slump of high strength concrete using neural network, Constr Build Mater. 20 (2006) 769–775. https://doi.org/10.1016/j.conbuildmat.2005.01.054.

[23] M.-Y. Cheng, J.-S. Chou, A.F.V. Roy, Y.-W. Wu, High-performance Concrete Compressive Strength Prediction using Time-Weighted Evolutionary Fuzzy Support Vector Machines Inference Model, Autom Constr. 28 (2012) 106–115. https://doi.org/10.1016/j.autcon.2012.07.004.

[24] C. Deepa, K. SathiyaKumari, V.P. Sudha, Prediction of the Compressive Strength of High Performance Concrete Mix using Tree Based Modeling, Int J Comput Appl. 6 (2010) 18–24. https://doi.org/10.5120/1076-1406.

[25] I.-C. Yeh, L.-C. Lien, Knowledge discovery of concrete material using Genetic Operation Trees, Expert Syst Appl. 36 (2009) 5807–5812. https://doi.org/10.1016/j.eswa.2008.07.004.

[26] A. Behnood, V. Behnood, M. Modiri Gharehveran, K.E. Alyamac, Prediction of the compressive strength of normal and high-performance concretes using M5P model tree algorithm, Constr Build Mater. 142 (2017) 199–207. https://doi.org/10.1016/j.conbuildmat.2017.03.061.

[27] S.-C. Lee, Prediction of concrete strength using artificial neural networks, Eng Struct. 25 (2003) 849–857. https://doi.org/10.1016/S0141-0296(03)00004-X.

[28] I.-C. Yeh, L.-C. Lien, Knowledge discovery of concrete material using Genetic Operation Trees, Expert Syst Appl. 36 (2009) 5807–5812. https://doi.org/10.1016/j.eswa.2008.07.004.

[29] I. Nunez, A. Marani, M. Flah, M.L. Nehdi, Estimating compressive strength of modern concrete mixtures using computational intelligence: A systematic review., Constr Build Mater. 310 (2021) 125279.

[30] T. Han, D. Jiang, Q. Zhao, L. Wang, K. Yin, Comparison of random forest, artificial neural networks and support vector machine for intelligent diagnosis of rotating machinery, Transactions of the Institute of Measurement and Control. 40 (2018) 2681–2693. https://doi.org/10.1177/0142331217708242.

[31] G. Ozcan, Y. Kocak, E. Gulbandilar, Estimation of compressive strength of BFS and WTRP blended cement mortars with machine learning models, Computers and Concrete. 19 (2017) 275–282. https://doi.org/10.12989/cac.2017.19.3.275.

[32] 饶炜东, Application of Machine Learning in the Prediction of Compressive Strength of Concrete, Statistics and Application. 06 (2017) 1–6. https://doi.org/10.12677/SA.2017.61001.

This is a preprint draft. The published article can be found at: https://doi.org/10.1016/j.istruc.2023.07.040.

Please cite this paper as:
Ghasemi A., Naser M.Z., (2023). "Tailoring 3D printed concrete through explainable artificial intelligence." *Structures*. https://doi.org/10.1016/j.istruc.2023.07.040.

[33] B. Khoshnevis, Automated construction by contour crafting—related robotics and information technologies, Autom Constr. 13 (2004) 5–19.

[34] H. Zhao, W. Sun, X. Wu, B. Gao, The effect of coarse aggregate gradation on the properties of self-compacting concrete, Mater Des. 40 (2012) 109–116.

[35] W. Ashraf, M. Noor, Performance-evaluation of concrete properties for different combined aggregate gradation approaches, Procedia Eng. 14 (2011) 2627–2634.

[36] J. Hu, A study of effects of aggregate on concrete rheology, Iowa State University. (2005).

[37] G. Ma, Z. Li, L. Wang, Printable properties of cementitious material containing copper tailings for extrusion based 3D printing, Constr Build Mater. 162 (2018) 613–627.

[38] Z. Malaeb, F. AlSakka, F. Hamzeh, 3D concrete printing: machine design, mix proportioning, and mix comparison between different machine setups, 3D Concrete Printing Technology. (2019) 115–136.

[39] S.H. Chu, L.G. Li, A.K.H. Kwan, Development of extrudable high strength fiber reinforced concrete incorporating nano calcium carbonate, Addit Manuf. 37 (2021) 101617. https://doi.org/10.1016/j.addma.2020.101617.

[40] T.T. Le, S.A. Austin, S. Lim, R.A. Buswell, A.G. Gibb, T. Thorpe, Mix design and fresh properties for high-performance printing concrete, Mater Struct. 45 (2012) 1221–1232.

[41] S. Lim, R.A. Buswell, T.T. Le, S.A. Austin, A.G.F. Gibb, T. Thorpe, Developments in construction-scale additive manufacturing processes, Autom Constr. 21 (2012) 262–268. https://doi.org/10.1016/j.autcon.2011.06.010.

[42] A. Perrot, D. Rangeard, A. Pierre, Structural built-up of cement-based materials used for 3D-printing extrusion techniques, Mater Struct. 49 (2016) 1213–1220.

[43] F. Bos, R. Wolfs, Z. Ahmed, T. Salet, Additive manufacturing of concrete in construction: potentials and challenges of 3D concrete printing, Virtual Phys Prototyp. 11 (2016) 209–225.

[44] A.M. Alhozaimy, Effect of absorption of limestone aggregates on strength and slump loss of concrete, Cem Concr Compos. 31 (2009) 470–473.

[45] https://www.chinesestandard.net/PDF.aspx/GBT14902-2012, (n.d.).

[46] https://www.chinesestandard.net/PDF/English.aspx/JGJT283-2012, (n.d.).

[47] https://www.chinesestandard.net/PDF/English.aspx/GBT2419-2005, (n.d.).

[48] L.G. Li, B.F. Xiao, Z.Q. Fang, Z. Xiong, S.H. Chu, A.K.H. Kwan, Feasibility of glass/basalt fiber reinforced seawater coral sand mortar for 3D printing, Addit Manuf. 37 (2021) 101684. https://doi.org/10.1016/j.addma.2020.101684.

[49] https://www.dimensions.ai/, (n.d.).

[50] J. Xiao, Z. Chen, T. Ding, S. Zou, Bending behaviour of steel cable reinforced 3D printed concrete in the direction perpendicular to the interfaces, Cem Concr Compos. 125 (2022) 104313.

[51] Z. Li, L. Wang, G. Ma, J. Sanjayan, D. Feng, Strength and ductility enhancement of 3D printing structure reinforced by embedding continuous micro-cables, Constr Build Mater. 264 (2020) 120196.

[52] L. Gebhard, J. Mata-Falcón, A. Anton, B. Dillenburger, W. Kaufmann, Structural behaviour of 3D printed concrete beams with various reinforcement strategies, Eng Struct. 240 (2021) 112380.

[53] B. Zhu, B. Nematollahi, J. Pan, Y. Zhang, Z. Zhou, Y. Zhang, 3D concrete printing of permanent formwork for concrete column construction, Cem Concr Compos. 121 (2021) 104039.

[54] B. Panda, S.C. Paul, M.J. Tan, Anisotropic mechanical performance of 3D printed fiber reinforced sustainable construction material, Mater Lett. 209 (2017) 146–149.

[55] M. Hambach, M. Rutzen, D. Volkmer, Properties of 3D-printed fiber-reinforced Portland cement paste, 3D Concrete Printing Technology. (2019) 73–113.

[56] F. Bos, E. Bosco, T. Salet, Ductility of 3D printed concrete reinforced with short straight steel fibers, Virtual Phys Prototyp. 14 (2019) 160–174.

[57] G. Ma, Z. Li, L. Wang, Printable properties of cementitious material containing copper tailings for extrusion based 3D printing, Constr Build Mater. 162 (2018) 613–627. https://doi.org/10.1016/j.conbuildmat.2017.12.051.

[58] F.P. Bos, E. Bosco, T.A.M. Salet, Ductility of 3D printed concrete reinforced with short straight steel fibers, Virtual Phys Prototyp. 14 (2019) 160–174. https://doi.org/10.1080/17452759.2018.1548069.

[59] B. Panda, S.C. Paul, M.J. Tan, Anisotropic mechanical performance of 3D printed fiber reinforced sustainable construction material, Mater Lett. 209 (2017) 146–149.

[60] Z. Li, L. Wang, G. Ma, J. Sanjayan, D. Feng, Strength and ductility enhancement of 3D printing structure reinforced by embedding continuous micro-cables, Constr Build Mater. 264 (2020) 120196.

[61] B. Zhu, B. Nematollahi, J. Pan, Y. Zhang, Z. Zhou, Y. Zhang, 3D concrete printing of permanent formwork for concrete column construction, Cem Concr Compos. 121 (2021) 104039.

[62] https://parametric-architecture.com/mars-architecture-studio-valentina-sumini/, (n.d.).

[63] I.-C. Yeh, MODELING OF STRENGTH OF HIGH-PERFORMANCE CONCRETE USING ARTIFICIAL NEURAL NETWORKS, Cem Concr Res. 28 (1998) 1797–1808.

[64] E.M. Golafshani, A. Behnood, M. Arashpour, Predicting the compressive strength of normal and High-Performance Concretes using ANN and ANFIS hybridized with Grey Wolf Optimizer, Constr Build Mater. 232 (2020) 117266.

[65] B. Vakhshouri, S. Nejadi, Prediction of compressive strength of self-compacting concrete by ANFIS models, Neurocomputing. 280 (2018) 13–22. https://doi.org/10.1016/j.neucom.2017.09.099.

[66] P. Chopra, R.K. Sharma, M. Kumar, Artificial Neural Networks for the Prediction of Compressive Strength of Concrete, International Journal of Applied Science and Engineering. 13 (2015) 187–204.

[67] https://scikit-learn.org/stable/, (n.d.).

[68] H.U. Abdullahi, A. Usman, S. Abba, Modelling the absorbance of a bioactive compound in HPLC method using artificial neural network and multilinear regression methods, Vol. 6 (2020) 362–371.

[69] M. Sergent, D. Mathieu, R. Phan-Tan-Luu, G. Drava, Correct and incorrect use of multilinear regression, Chemometrics and Intelligent Laboratory Systems. 27 (1995) 153–162. https://doi.org/10.1016/0169-7439(95)80020-A.

[70] W.-B. Chen, W.-C. Liu, Water quality modeling in reservoirs using multivariate linear regression and two neural network models, Advances in Artificial Neural Systems. (2015).

[71] https://www.geeksforgeeks.org/xgboost-for-regression/, (n.d.).

[72] J. Pesantez-Narvaez, M. Guillen, M. Alcañiz, Predicting motor insurance claims using telematics data—XGBoost versus logistic regression, Risks. 7 (2019) 70.

[73] L. Breiman, Random forests, Mach Learn. 45 (2001) 5–32.

[74] H.-V.T. Mai, T.-A. Nguyen, H.-B. Ly, V.Q. Tran, Prediction Compressive Strength of Concrete Containing GGBFS using Random Forest Model, Advances in Civil Engineering. 2021 (2021) 1–12. https://doi.org/10.1155/2021/6671448.

[75] K.J. Archer, R. v Kimes, Empirical characterization of random forest variable importance measures, Computational Statistics & Data Analysi. 52 (2008) 2249–2260.

[76] A. Tapeh, M.Z. Naser, Artificial Intelligence, Machine Learning, and Deep Learning in Structural Engineering: A Scientometrics Review of Trends and Best Practices, Archives of Computational Methods in Engineering. (2022).

[77] T. Fushiki, Estimation of prediction error by using K-fold cross-validation, Stat Comput. 21 (2011) 137–146. https://doi.org/10.1007/s11222-009-9153-8.

[78] R. Couronné, P. Probst, A.-L. Boulesteix, Random forest versus logistic regression: a large-scale benchmark experiment, BMC Bioinformatics. 19 (2018) 270. https://doi.org/10.1186/s12859-018-2264-5.

[79] https://scikit-learn.org/stable/modules/cross_validation.html, (n.d.).

[80] M.Z. Naser, A. Alavi, Error metrics and performance fitness indicators for artificial intelligence and machine learning in engineering and sciences, Architecture, Structures and Construction. (2021).

[81] S. Yu, J. Sanjayan, H. Du, Effects of cement mortar characteristics on aggregate-bed 3D concrete printing, Addit Manuf. 58 (2022) 103024. https://doi.org/10.1016/j.addma.2022.103024.

[82] H.A.A. Diniz, A.E. Martinelli, K.C. Cabral, R.L. da S. Ferreira, I.F.D. da Silva, Synergistic effects of the use of metakaolin, sand and water on the properties of cementitious composites for 3D printing, Constr Build Mater. 366 (2023) 130277. https://doi.org/10.1016/j.conbuildmat.2022.130277.

[83] J.H. Friedman, Greedy function approximation: a gradient boosting machine, Ann Stat. (2001) 1189–1232.

[84] https://towardsdatascience.com/explainable-ai-xai-methods-part-3-accumulated-local-effects-ale-cf6ba3387fde, (n.d.).

[85] https://stackoverflow.com/questions/46596945/interpreting-y-axis-of-partial-dependence-plots-produced-by-pdp-package, (n.d.).

[86] U. Kamath, J. Liu, Explainable Artificial Intelligence: An Introduction to Interpretable Machine Learning, Springer, 2021.

[87] N. Khalil, G. Aouad, K. el Cheikh, S. Rémond, Use of calcium sulfoaluminate cements for setting control of 3D-printing mortars, Constr Build Mater. 157 (2017) 382–391. https://doi.org/10.1016/j.conbuildmat.2017.09.109.

[88] P. Shakor, S. Nejadi, G. Paul, A Study into the Effect of Different Nozzles Shapes and Fibre-Reinforcement in 3D Printed Mortar, Materials. 12 (2019) 1708. https://doi.org/10.3390/ma12101708.

[89] V.N. Nerella, V. Mechtcherine, Studying the printability of fresh concrete for formwork-free concrete onsite 3D printing technology (CONPrint3D), 3D Concrete Printing Technology. (2019) 333–347.

[90] M.-I. Álvarez-Fernández, M.-B. Prendes-Gero, C. González-Nicieza, D.-J. Guerrero-Miguel, J.E. Martínez-Martínez, Optimum Mix Design for 3D Concrete Printing Using Mining Tailings: A Case Study in Spain, Sustainability. 13 (2021) 1568. https://doi.org/10.3390/su13031568.

[91] T. Ding, F. Qin, J. Xiao, X. Chen, Z. Zuo, Experimental study on the bond behaviour between steel bars and 3D printed concrete, Journal of Building Engineering. 49 (2022) 104105. https://doi.org/10.1016/j.jobe.2022.104105.

[92] A.V. Rahul, M. Santhanam, H. Meena, Z. Ghani, Mechanical characterization of 3D printable concrete, Constr Build Mater. 227 (2019) 116710. https://doi.org/10.1016/j.conbuildmat.2019.116710.

[93] P. Shakor, S. Nejadi, S. Sutjipto, G. Paul, N. Gowripalan, Effects of deposition velocity in the presence/absence of E6-glass fibre on extrusion-based 3D printed mortar, Addit Manuf. 32 (2020) 101069. https://doi.org/10.1016/j.addma.2020.101069.

[94] A. Ting, D. Tay, A. Annapareddy, M. Li, M. Tan, Effect of recycled glass gradation in 3D cementitious material printing, Proc. 3rd Int. Conf. Prog. Addit. Manuf.(Pro-AM 2018). (2018) 50–55.

[95] A. Kazemian, X. Yuan, E. Cochran, B. Khoshnevis, Cementitious materials for construction-scale 3D printing: Laboratory testing of fresh printing mixture, Constr Build Mater. 145 (2017) 639–647. https://doi.org/10.1016/j.conbuildmat.2017.04.015.

[96] M. van den Heever, F. Bester, J. Kruger, G. van Zijl, Mechanical characterisation for numerical simulation of extrusion-based 3D concrete printing, Journal of Building Engineering. 44 (2021) 102944. https://doi.org/10.1016/j.jobe.2021.102944.

[97] F. Bos, R. Wolfs, Z. Ahmed, T. Salet, Additive manufacturing of concrete in construction: potentials and challenges of 3D concrete printing, Virtual Phys Prototyp. 11 (2016) 209–225. https://doi.org/10.1080/17452759.2016.1209867.

[98] N. Hack, I. Dressler, L. Brohmann, S. Gantner, D. Lowke, H. Kloft, Injection 3D Concrete Printing (I3DCP): Basic Principles and Case Studies, Materials. 13 (2020) 1093. https://doi.org/10.3390/ma13051093.

[99] T.S. Rushing, G. Al-Chaar, B.A. Eick, J. Burroughs, J. Shannon, L. Barna, M. Case, Investigation of concrete mixtures for additive construction, Rapid Prototyp J. 23 (2017) 74–80. https://doi.org/10.1108/RPJ-09-2015-0124.

[100] B. Panda, S. Ruan, C. Unluer, M.J. Tan, Improving the 3D printability of high volume fly ash mixtures via the use of nano attapulgite clay, Compos B Eng. 165 (2019) 75–83. https://doi.org/10.1016/j.compositesb.2018.11.109.

[101] J. van der Putten, D. Snoeck, K. van Tittelboom, 3D Printing of cementitious materials with superabsorbent polymers, Durable Concrete for Infrastructure under Severe Conditions-Smart Admixtures, Self-Responsiveness and Nano-Additions. (2019) 86–89.

[102] D. Lee, B.-H. Yoo, H.-J. Son, Development of Shrinkage Reducing Agent for 3D Printing Concrete, Journal of the Korea Academia-Industrial Cooperation Society. 20 (2019) 37–43.

[103] I. Dressler, N. Freund, D. Lowke, The Effect of Accelerator Dosage on Fresh Concrete Properties and on Interlayer Strength in Shotcrete 3D Printing, Materials. 13 (2020) 374. https://doi.org/10.3390/ma13020374.

[104] J.J. Assaad, F. Hamzeh, B. Hamad, Qualitative assessment of interfacial bonding in 3D printing concrete exposed to frost attack, Case Studies in Construction Materials. 13 (2020) e00357. https://doi.org/10.1016/j.cscm.2020.e00357.

[105] A. Perrot, M&S highlight: Le et al. (2012), Mix design and fresh properties for high-performance printing concrete, Mater Struct. 55 (2022) 42. https://doi.org/10.1617/s11527-021-01855-y.

[106] C. Joh, J. Lee, T.Q. Bui, J. Park, I.-H. Yang, Buildability and Mechanical Properties of 3D Printed Concrete, Materials. 13 (2020) 4919. https://doi.org/10.3390/ma13214919.

[107] M. Meurer, M. Classen, Mechanical Properties of Hardened 3D Printed Concretes and Mortars—Development of a Consistent Experimental Characterization Strategy, Materials. 14 (2021) 752. https://doi.org/10.3390/ma14040752.

[108] V.N. Nerella, S. Hempel, V. Mechtcherine, Effects of layer-interface properties on mechanical performance of concrete elements produced by extrusion-based 3D-printing, Constr Build Mater. 205 (2019) 586–601. https://doi.org/10.1016/j.conbuildmat.2019.01.235.

[109] B. Panda, S.C. Paul, N.A.N. Mohamed, Y.W.D. Tay, M.J. Tan, Measurement of tensile bond strength of 3D printed geopolymer mortar, Measurement. 113 (2018) 108–116. https://doi.org/10.1016/j.measurement.2017.08.051.

[110] B. Baz, G. Aouad, S. Remond, Effect of the printing method and mortar's workability on pull-out strength of 3D printed elements, Constr Build Mater. 230 (2020) 117002. https://doi.org/10.1016/j.conbuildmat.2019.117002.

[111] A. Singh, Q. Liu, J. Xiao, Q. Lyu, Mechanical and macrostructural properties of 3D printed concrete dosed with steel fibers under different loading direction, Constr Build Mater. 323 (2022) 126616. https://doi.org/10.1016/j.conbuildmat.2022.126616.

[112] T. Ding, J. Xiao, S. Zou, Y. Wang, Hardened properties of layered 3D printed concrete with recycled sand, Cem Concr Compos. 113 (2020) 103724. https://doi.org/10.1016/j.cemconcomp.2020.103724.

[113] T. Ding, J. Xiao, F. Qin, Z. Duan, Mechanical behavior of 3D printed mortar with recycled sand at early ages, Constr Build Mater. 248 (2020) 118654. https://doi.org/10.1016/j.conbuildmat.2020.118654.

[114] H. Kloft, H.-W. Krauss, N. Hack, E. Herrmann, S. Neudecker, P.A. Varady, D. Lowke, Influence of process parameters on the interlayer bond strength of concrete elements additive manufactured by Shotcrete 3D Printing (SC3DP), Cem Concr Res. 134 (2020) 106078. https://doi.org/10.1016/j.cemconres.2020.106078.

[115] A.V. Rahul, M. Santhanam, Evaluating the printability of concretes containing lightweight coarse aggregates, Cem Concr Compos. 109 (2020) 103570. https://doi.org/10.1016/j.cemconcomp.2020.103570.

[116] V. Mechtcherine, V.N. Nerella, F. Will, M. Näther, J. Otto, M. Krause, Large-scale digital concrete construction – CONPrint3D concept for on-site, monolithic 3D-printing, Autom Constr. 107 (2019) 102933. https://doi.org/10.1016/j.autcon.2019.102933.

[117] A.L. van Overmeir, S.C. Figueiredo, B. Šavija, F.P. Bos, E. Schlangen, Design and analyses of printable strain hardening cementitious composites with optimized particle size distribution, Constr Build Mater. 324 (2022) 126411. https://doi.org/10.1016/j.conbuildmat.2022.126411.

[118] S. Cho, P. Kruger, S. Zeranka, G. van Zijl, Concr. Bet, 3D printable concrete technology and mechanics, Concr. Bet. 158 (2019) 11–18.

[119] J. Kruger, M. van den Heever, S. Cho, S. Zeranka, G. van Zijl, HIGH-PERFORMANCE 3D PRINTABLE CONCRETE ENHANCED WITH NANOMATERIALS, Proceedings of the International Conference on Sustainable Materials, Systems and Structures (SMSS 2019). 533 (2019).

[120] C. Liu, R. Zhang, H. Liu, C. He, Y. Wang, Y. Wu, S. Liu, L. Song, F. Zuo, Analysis of the mechanical performance and damage mechanism for 3D printed concrete based on pore structure, Constr Build Mater. 314 (2022) 125572. https://doi.org/10.1016/j.conbuildmat.2021.125572.

[121] Y. Tao, A.V. Rahul, K. Lesage, K. van Tittelboom, Y. Yuan, G. de Schutter, Mechanical and microstructural properties of 3D printable concrete in the context of the twin-pipe pumping strategy, Cem Concr Compos. 125 (2022) 104324. https://doi.org/10.1016/j.cemconcomp.2021.104324.

[122] J. Ye, C. Cui, J. Yu, K. Yu, F. Dong, Effect of polyethylene fiber content on workability and mechanical-anisotropic properties of 3D printed ultra-high ductile concrete, Constr Build Mater. 281 (2021) 122586. https://doi.org/10.1016/j.conbuildmat.2021.122586.

[123] L. Ma, Q. Zhang, Z. Jia, C. Liu, Z. Deng, Y. Zhang, Effect of drying environment on mechanical properties, internal RH and pore structure of 3D printed concrete, Constr Build Mater. 315 (2022) 125731. https://doi.org/10.1016/j.conbuildmat.2021.125731.

[124] B. Baz, G. Aouad, N. Khalil, S. Remond, Inter-layer reinforcement of 3D printed concrete elements, Asian Journal of Civil Engineering. 22 (2021) 341–349. https://doi.org/10.1007/s42107-020-00317-0.

[125] A.V. Rahul, M.K. Mohan, G. de Schutter, K. van Tittelboom, 3D printable concrete with natural and recycled coarse aggregates: Rheological, mechanical and shrinkage behaviour, Cem Concr Compos. 125 (2022) 104311. https://doi.org/10.1016/j.cemconcomp.2021.104311.

[126] G. Ji, J. Xiao, P. Zhi, Y.-C. Wu, N. Han, Effects of Extrusion Parameters on Properties of 3d Printing Concrete with Coarse Aggregates, SSRN Electronic Journal. (2021). https://doi.org/10.2139/ssrn.3974338.

[127] Chen, Li, Chaves Figueiredo, Çopuroğlu, Veer, Schlangen, Limestone and Calcined Clay-Based Sustainable Cementitious Materials for 3D Concrete Printing: A Fundamental Study of Extrudability and Early-Age Strength Development, Applied Sciences. 9 (2019) 1809. https://doi.org/10.3390/app9091809.

[128] J.H. Jo, B.W. Jo, W. Cho, J.-H. Kim, Development of a 3D Printer for Concrete Structures: Laboratory Testing of Cementitious Materials, Int J Concr Struct Mater. 14 (2020) 13. https://doi.org/10.1186/s40069-019-0388-2.

[129] S.R. Wang, X.G. Wu, J.H. Yang, J.Q. Zhao, F.L. Kong, Mechanical behavior of lightweight concrete structures subjected to 3D coupled static–dynamic loads, Acta Mech. 231 (2020) 4497–4511. https://doi.org/10.1007/s00707-020-02739-y.

[130] W.-J. Long, J.-L. Tao, C. Lin, Y. Gu, L. Mei, H.-B. Duan, F. Xing, Rheology and buildability of sustainable cement-based composites containing micro-crystalline cellulose for 3D-printing, J Clean Prod. 239 (2019) 118054. https://doi.org/10.1016/j.jclepro.2019.118054.

[131] J. Xiao, Z. Lv, Z. Duan, S. Hou, Study on preparation and mechanical properties of 3D printed concrete with different aggregate combinations, Journal of Building Engineering. 51 (2022) 104282. https://doi.org/10.1016/j.jobe.2022.104282.

[132] M. Kaszyńska, S. Skibicki, M. Hoffmann, 3D Concrete Printing for Sustainable Construction, Energies (Basel). 13 (2020) 6351. https://doi.org/10.3390/en13236351.

[133] K. Yu, W. McGee, T.Y. Ng, H. Zhu, V.C. Li, 3D-printable engineered cementitious composites (3DP-ECC): Fresh and hardened properties, Cem Concr Res. 143 (2021) 106388. https://doi.org/10.1016/j.cemconres.2021.106388.

[134] L. Pham, G. Lu, P. Tran, Influences of Printing Pattern on Mechanical Performance of Three-Dimensional-Printed Fiber-Reinforced Concrete, 3D Print Addit Manuf. 9 (2022) 46–63. https://doi.org/10.1089/3dp.2020.0172.

[135] K. Federowicz, M. Kaszyńska, A. Zieliński, M. Hoffmann, Effect of Curing Methods on Shrinkage Development in 3D-Printed Concrete, Materials. 13 (2020) 2590. https://doi.org/10.3390/ma13112590.

[136] H. Cui, S. Yu, X. Cao, H. Yang, Evaluation of Printability and Thermal Properties of 3D Printed Concrete Mixed with Phase Change Materials, Energies (Basel). 15 (2022) 1978. https://doi.org/10.3390/en15061978.

This is a preprint draft. The published article can be found at: https://doi.org/10.1016/j.istruc.2023.07.040.

Please cite this paper as:
Ghasemi A., Naser M.Z., (2023). "Tailoring 3D printed concrete through explainable artificial intelligence." *Structures*. https://doi.org/10.1016/j.istruc.2023.07.040.

Appendix A

Table A1. Database used in this study. This database will be provided upon the publication of this paper.

Ref.	Cement (Kg)	Water (Kg)	Silica fume	SP (%)	Fine Agg.	Fly ash	Age	CS
Khalil, et al.[87]	683	236	0	0.25	850	0	7	70
	675	236	0	0.26	850	0	7	78
	682	236	0	0.25	850	0	28	87
	675	236	0	0.26	850	0	28	86
	683	236	0	0.25	850	0	56	85
	675	236	0	0.26	850	0	56	91
Shakor, et al. [88]	375	125	0	0.66	375	0	7	56.42
	375	125	0	0.66	375	0	7	63.12
	375	125	0	0.66	375	0	28	59.7
	375	125	0	0.66	375	0	28	68.95
Nerella, et al. [89]	430	180	180	1.2	1240	170	3	49.7
	430	180	180	1.2	1240	170	21	80.6
Rahul, et al. [6]	573.6	262.2	81.9	0.17	491.7	164	28	70.9
	663	265.2	2.47	0.13	497.2	165.7	28	71.7
	663	265.2	0.82	0.18	497.2	165.7	28	67.4
Alvarez-Fernandez, et al. [90]	12	29	0	0	0	0	28	0.9
	13	20	0	0	0	0	28	3.3
	24	18	0	0	0	0	28	9.3
	24	17	0	0	36	0	28	13.4
	24	15	0	0	48	0	28	23.5
Ding, et al. [91]	1000	350	0	0.071	1000	0	28	42.03
	1000	420	0	0.086	1000	0	28	43.04
	1000	350	0	0.09	1000	0	28	46.74
	1000	420	0	0.095	1000	0	28	34.01
Rahul, et al. [92]	574	262	82	34	1230	164	7	55
	663	265	0	34	1243	166	7	54
	663	265	0	34	1486	166	7	52
Shakor, et al. [93]	5.06	1.89	0	0.5	6.075	0	28	14.91
	5.06	1.89	0	0.5	6.075	0	28	23.34
	5.06	1.89	0	0.5	6.075	0	28	13.83
	5.06	1.89	0	0.5	6.075	0	28	13.43
	5.06	1.89	0	0.5	6.075	0	28	50.82
	5.06	1.89	0	0.59	6.075	0	28	31.09
	5.06	1.89	0	0.59	6.075	0	28	28.25

	5.06	1.89	0	0.59	6.075	0	28	25.37
	5.06	1.89	0	0.59	6.075	0	28	25.33
	5.06	1.89	0	0.59	6.075	0	28	51.92
Annapareddy, et al. [94]	138	120	12	0	243	122.4	7	19
	138	120	12	0	243	122.4	7	19
	138	906.9	12	0	221.7	122.4	7	22
Kazemian, et al. [95]	600	259	0	0.05	1379	0	7	32.9
	540	259	60	0.16	1357	0	7	35.2
	600	259	0	0.06	1379	0	7	31
	600	259	0	0.15	1379	0	7	31.8
	600	259	0	0.05	1379	0	28	44.7
	540	259	60	0.16	1357	0	28	49.9
	600	259	0	0.06	1379	0	28	45.1
	600	259	0	0.15	1379	0	28	45.9
Heever, et al. [96]	562	256	81.4	0.6	1144	162	28	38.2
Bos, et al. [97]	37.5	144	0	0	48	0	0	40.6
	37.5	126	0	0	48	0	0	41.5
	37.5	117	0	0	48	0	0	42.3
	37.5	114	0	0	48	0	0	43.5
	37.5	108	0	0	48	0	0	55.4
Hack, et al. [98]	595.1	342.8	27.1	0	1064	0	2	59.3
Rushing, et al. [99]	300	141	0	0	690	0	0	40.5
Panda, et al. [100]	300	350	250	0	1220	675	28	31.3
Van Der Putten, et al. [101]	620.5	226.5	0	0	1241	0	0	62
Lee, et al. [102]	289	168	0	1.1	899	51	1	6
	289	168	0	1	899	51	1	6.8
	289	168	0	0.95	899	51	1	6.9
	289	168	0	1.1	899	51	1	6.1
	289	168	0	1.1	899	51	1	6
	289	168	0	1.05	899	51	1	7
	289	168	0	1.25	899	51	1	7.5
	289	168	0	1.1	899	51	1	7.3
	289	168	0	1.1	899	51	7	28.5
	289	168	0	1	899	51	7	28
	289	168	0	0.95	899	51	7	28.1
	289	168	0	1.1	899	51	7	25.1
	289	168	0	1.1	899	51	7	28.1
	289	168	0	1.05	899	51	7	25.3
	289	168	0	1.25	899	51	7	28.1

	289	168	0	1.1	899	51	7	30
	289	168	0	1.1	899	51	28	37
	289	168	0	1	899	51	28	37
	289	168	0	0.95	899	51	28	36.9
	289	168	0	1.1	899	51	28	35.5
	289	168	0	1.1	899	51	28	36
	289	168	0	1.05	899	51	28	35.5
	289	168	0	1.25	899	51	28	36.9
	289	168	0	1.1	899	51	28	40
	588	235	84	2	936	168	1	17
	588	235	84	2.1	936	168	1	20.5
	588	235	84	2.05	936	168	1	21
	588	235	84	2	936	168	7	31
	588	235	84	2.1	936	168	7	50
	588	235	84	2.05	936	168	7	51
	588	235	84	2	936	168	28	64
	588	235	84	2.1	936	168	28	70
	588	235	84	2.05	936	168	28	72
Dressler, et al. [103]	600	270	0	0.3	1258	0	28	59.9
	600	270	0	0.3	1258	0	28	64.8
	600	270	0	0.3	1258	0	28	66
	600	270	0	0.3	1258	0	28	65.7
Assaad, et al. [104]	506	247.5	44	2.1	0	0	28	42.5
	506	247.5	44	1.9	0	0	28	30.6
	506	247.5	44	1.8	0	0	28	37.9
	598	292.5	52	0.95	0	0	28	51.3
	598	292.5	52	0.9	0	0	28	39.8
	598	292.5	52	0.8	0	0	28	47.7
	690	262.5	60	1.25	0	0	28	66.7
	690	262.5	60	1.15	0	0	28	46.2
	690	262.5	60	1.0	0	0	28	62.6
Le, et al. [105]	579	216	83	1	1241	165	1	20
	579	216	83	1	1241	165	7	80
	579	216	83	1	1241	165	28	110
	579	216	83	1	1241	165	56	125
Weng, et al. [9]	300	90	30	8.19	150	300	7	31
	300	90	30	8.19	150	300	7	27
	300	90	30	8.19	150	300	7	36
	300	90	30	8.19	150	300	7	28
	300	90	30	8.19	150	300	7	35

This is a preprint draft. The published article can be found at: https://doi.org/10.1016/j.istruc.2023.07.040.

Please cite this paper as:
Ghasemi A., Naser M.Z., (2023). "Tailoring 3D printed concrete through explainable artificial intelligence." *Structures*. https://doi.org/10.1016/j.istruc.2023.07.040.

	300	90	30	8.19	150	300	7	34
	300	90	30	8.19	150	300	14	37
	300	90	30	8.19	150	300	14	35
	300	90	30	8.19	150	300	14	39
	300	90	30	8.19	150	300	14	36
	300	90	30	8.19	150	300	14	41
	300	90	30	8.19	150	300	14	38
	300	90	30	8.19	150	300	28	50
	300	90	30	8.19	150	300	28	42
	300	90	30	8.19	150	300	28	51
	300	90	30	8.19	150	300	28	41
	300	90	30	8.19	150	300	28	45
	300	90	30	8.19	150	300	28	60
Joh, et al. [106]	576	240	79	1	1154	172	28	23.5
Meurer, et al. [107]	550	280	0	0	1172	250	22	65.8
Nerella, et al. [108]	627	263.34	0	0.75	1391	0	1.00	41.9
	627	263.34	0	0.75	1391	0	28.00	64.5
	391	164.22	213	2	1260	213	1.00	28.3
	391	164.22	213	2	1260	213	28.00	97.9
Panda, et al. [109]	0	144.09	101.86	1.40	1220.00	572.34	28.00	36.00
Baz, et al. [110]	614	273	68	0.26	850	0	3	30.00
	614	273	68	0.36	850	0	3	27.1
	614	273	68	0.4	850	0	3	29.6
	614	306	68	0.4	850	0	3	25.1
	614	273	68	0.26	850	0	28	49.1
	614	273	68	0.36	850	0	28	46.6
	614	273	68	0.4	850	0	28	46.5
	614	306	68	0.4	850	0	28	46.7
Singh, et al. [111]	1000.0	350.00	0	0.08	1000.00	0	28.00	30.0
	1000.0	350.00	0	0.087	1000.00	0	28.00	26.3
	1000.0	350.00	0	0.115	1000.00	0	28.00	29.5
	1000.0	350.00	0	0.132	1000.00	0	28.00	33.5
	1000.0	350.00	0	0.152	1000.00	0	28.00	30.5
Ding, et al. [112]	1000.00	350.00	0	0.083	1000.00	0	28.0	21.5
	1000.00	361.25	0	0.103	875.00	0	28.0	28.5
	1000.00	372.50	0	0.125	750.00	0	7.0	11.0
	1000.00	372.50	0	0.125	750.00	0	14.0	15.6
	1000.00	372.50	0	0.125	750.00	0	28.0	19.3
	1000.00	395.00	0	0.185	500.00	0	28.0	18.0
Ding, et al. [113]	1000.0	350.0	0	0.071	1000.0	0	0.104	0.030

This is a preprint draft. The published article can be found at: https://doi.org/10.1016/j.istruc.2023.07.040.

Please cite this paper as:
Ghasemi A., Naser M.Z., (2023). "Tailoring 3D printed concrete through explainable artificial intelligence." *Structures*. https://doi.org/10.1016/j.istruc.2023.07.040.

	1000.0	385.0	0	0.074	750.0	0	0.104	0.042
	1000.0	420.0	0	0.086	500.0	0	0.104	0.045
Kloft, et al. [114]	500.00	160.00	25.00	0.77	1180.00	0	14.0	56.9
	500.00	160.00	25.00	0.77	1180.00	0	28.0	59.3
Rahul, et al. [115]	660.00	264.00	0	0.08	1237.00	165.00	0.041	0.0050
	660.00	264.00	0	0.08	1237.00	165.00	0.083	0.0064
	660.00	264.00	0	0.08	1237.00	165.00	0.125	0.0079
	612.00	245.00	0	0.08	938.00	153.00	0.041	0.0078
	612.00	245.00	0	0.08	938.00	153.00	0.083	0.0100
	612.00	245.00	0	0.08	938.00	153.00	0.125	0.0137
Mechtcherine, et al. [116]	350.00	179.00	0	1.02	1179.00	140.00	10.00	46.9
Overmeir, et al. [117]	483.00	347.00	70.00	0.26	284.00	0	7.00	32.00
	483.00	347.00	70.00	0.26	284.00	0	14.00	46.5
	483.00	347.00	70.00	0.26	284.00	0	28.00	51.0
	458.00	355.00	51.00	0.24	549.00	0	7.00	32.00
	458.00	355.00	51.00	0.24	549.00	0	14.00	44.0
	458.00	355.00	51.00	0.24	549.00	0	28.00	56.0
Cho, et al. [118]	579.00	261.00	83.00	1.48	1167.00	165.00	1.00	7.9
	579.00	261.00	83.00	1.48	1167.00	165.00	7.00	55.6
	579.00	261.00	83.00	1.48	1167.00	165.00	28.00	70.6
	579.00	261.00	83.00	1.48	1167.00	165.00	56.00	80.0
Kruger, et al.	579.00	261.00	83.0	1.48	1167.00	165.0	1.0	8.1
[119]	579.00	261.00	83.0	1.48	1167.00	165.0	7.0	58.5
	579.00	261.00	83.0	1.48	1167.00	165.0	28.0	74.3
	579.00	261.00	83.0	1.48	1167.00	165.0	56.0	78.2
Liu, et al. [120]	756.40	226.92	24.40	0.35	1220.00	48.80	1.00	13.28
	756.40	226.92	24.40	0.35	1220.00	48.80	4.00	21.54
	756.40	226.92	24.40	0.35	1220.00	48.80	7.00	23.62
	756.40	226.92	24.40	0.35	1220.00	48.80	14.00	24.44
	756.40	226.92	24.40	0.35	1220.00	48.80	28.00	26.87
Tao, et al. [121]	1069.41	300.90	0	0.53	969.60	0	3.0	19.0
	0	396.31	0	0	912.57	0	3.0	18.5
	712.94	332.71	0	0.79	950.59	0	3.0	19.0
	1069.41	300.90	0	0.53	969.60	0	7.0	25.5
	0.0	396.31	0	0	912.57	0	7.0	24.5
	712.94	332.71	0	0.79	950.59	0	7.0	25.7
	1069.41	300.90	0	0.53	969.60	0	28.0	35.5
	0.0	396.31	0	0	912.57	0	28.0	35.0
	712.94	332.71	0	0.79	950.59	0	28.0	35.7

This is a preprint draft. The published article can be found at: https://doi.org/10.1016/j.istruc.2023.07.040.

Please cite this paper as:
Ghasemi A., Naser M.Z., (2023). "Tailoring 3D printed concrete through explainable artificial intelligence." *Structures*. https://doi.org/10.1016/j.istruc.2023.07.040.

Xiao, et al. [121]	320.00	112.00	0	0.075	320.00	0	28.00	24.00
	320.00	134.00	0	0.084	160.00	0	28.00	17.00
	320.00	112.00	0	0.131	320.00	0	28.00	34.00
	320.00	134.00	0	0.153	160.00	0	28.00	28.50
	320.00	112.00	0	0.075	320.00	0	28.00	32.00
Ye, et al. [122]	656.00	275.4	246.00	0.294	246.00	118.00	28.00	39.80
Ma, et al. [123]	702.7	229.1	61.1	0.17	1222.0	0	3.0	41.5
	702.7	229.1	61.1	0.17	1222.0	0	7.0	51.3
	702.7	229.1	61.1	0.17	1222.0	0	28.0	57.0
Baz, et al. [124]	614.00	245.60	68.00	0.26	850.00	0	3.0	24.00
	614.00	245.60	68.00	0.26	850.00	0	7.0	30.00
	614.00	245.60	68.00	0.26	850.00	0	28.0	46.00
Rahul, et al. [125]	376.3	263.4	0	1.4	1279.3	0	28.00	35.00
	374.2	261.9	0	0.99	900.8	0	28.00	32.00
	370.8	259.6	0	0.90	909.4	0	28.00	31.00
Ji, et al. [126]	444.00	210.00	41.4	0.09	870.00	96.6	28.00	34.5
Chen, et al. [127]	331.00	248.00	0	2.05	1242.00	0	1.00	1.0
	331.00	248.00	0	2.05	1242.00	0	1.00	6.5
	331.00	248.00	0	2.05	1242.00	0	1.00	10.7
	331.00	248.00	0	2.27	1242.00	0	1.00	15.00
	331.00	248.00	0	2.05	1242.00	0	7.00	12.5
	331.00	248.00	0	2.05	1242.00	0	7.00	25.7
	331.00	248.00	0	2.05	1242.00	0	7.00	34.5
	331.00	248.00	0	2.27	1242.00	0	7.00	35.00
	331.00	248.00	0	2.05	1242.00	0	28.00	13.00
	331.00	248.00	0	2.05	1242.00	0	28.00	34.7
	331.00	248.00	0	2.05	1242.00	0	28.00	39.00
	331.00	248.00	0	2.27	1242.00	0	28.00	45.7
Jo, et al. [128]	300.00	92.25	0	0	525.00	0	0	60.4
	300.00	84.55	0	0	477.27	0	0	62.00
Wang, et al. [129]	481.00	171.00	0	2.0	408.00	157.00	28.00	31.00
Long, et al. [130]	780.00	455.00	130.00	0.35	130.00	390.00	3.00	25.00
	780.00	455.00	130.00	0.35	130.00	390.00	3.00	26.00
	780.00	455.00	130.00	0.35	130.00	390.00	3.00	28.00
	780.00	455.00	130.00	0.35	130.00	390.00	3.00	26.0
	780.00	455.00	130.00	0.35	130.00	390.00	3.00	37.00
	780.00	455.00	130.00	0.35	130.00	390.00	7.0	40.00
	780.00	455.00	130.00	0.35	130.00	390.00	7.0	44.00
	780.00	455.00	130.00	0.35	130.00	390.00	7.0	59.00

This is a preprint draft. The published article can be found at: https://doi.org/10.1016/j.istruc.2023.07.040.

Please cite this paper as:
Ghasemi A., Naser M.Z., (2023). "Tailoring 3D printed concrete through explainable artificial intelligence." *Structures*. https://doi.org/10.1016/j.istruc.2023.07.040.

	780.00	455.00	130.00	0.35	130.00	390.00	7.0	44.00
	780.00	455.00	130.00	0.35	130.00	390.00	7.0	50.00
	780.00	455.00	130.00	0.35	130.00	390.00	28.0	48.00
	780.00	455.00	130.00	0.35	130.00	390.00	28.0	51.00
	780.00	455.00	130.00	0.35	130.00	390.00	28.0	57.00
	780.00	455.00	130.00	0.35	130.00	390.00	28.0	52.5
	780.00	455.00	130.00	0.35	130.00	390.00	28.0	57.5
Xiao, et al. [131]	444.00	210.00	41.4	0.15	870.00	96.6	7.00	31.00
	444.00	231.37	41.4	0.20	870.00	96.6	7.00	22.5
	444.00	254.09	41.4	0.22	818.00	96.6	7.00	21.00
	444.00	275.46	41.4	0.30	818.00	96.6	7.00	17.50
	444.00	210.00	41.4	0.15	870.00	96.6	28.00	47.50
	444.00	231.37	41.4	0.20	870.00	96.6	28.00	32.50
	444.00	254.09	41.4	0.22	818.00	96.6	28.00	30.00
	444.00	275.46	41.4	0.30	818.00	96.6	28.00	24.00
Kaszynska, et al. [132]	588.00	232.00	84.00	0.23	989.00	168.00	0.41	17.00
	588.00	232.00	84.00	0.19	1233.00	168.00	0.41	16.00
	840.00	232.00	0.00	0.21	1047.00	0.00	0.41	16.5
	840.00	232.00	0.00	0.05	1304.00	0.00	0.41	16.00
	448.00	179.2	64.00	0.34	1258.00	128.00	0.41	8.00
	448.00	179.2	64.00	0.40	1568.00	128.00	0.41	5.00
	640.00	179.2	0.00	0.32	1302.00	0.00	0.41	7.00
	640.00	179.2	0.00	0.28	1623.00	0.00	0.41	7.5
	588.00	232.00	84.00	0.23	989.00	168.00	1.00	42.00
	588.00	232.00	84.00	0.19	1233.00	168.00	1.00	52.00
	840.00	232.00	0.00	0.21	1047.00	0.00	1.00	38.00
	840.00	232.00	0.00	0.05	1304.00	0.00	1.00	37.00
	448.00	179.2	64.00	0.34	1258.00	128.00	1.00	36.00
	448.00	179.2	64.00	0.40	1568.00	128.00	1.00	30.00
	640.00	179.2	0.00	0.32	1302.00	0.00	1.00	28.00
	640.00	179.2	0.00	0.28	1623.00	0.00	1.00	38.00
	588.00	232.00	84.00	0.23	989.00	168.00	3.00	62.00
	588.00	232.00	84.00	0.19	1233.00	168.00	3.00	76.00
	840.00	232.00	0.00	0.21	1047.00	0.00	3.00	51.00
	840.00	232.00	0.00	0.05	1304.00	0.00	3.00	62.00
	448.00	179.2	64.00	0.34	1258.00	128.00	3.00	47.00
	448.00	179.2	64.00	0.40	1568.00	128.00	3.00	43.00
	640.00	179.2	0.00	0.32	1302.00	0.00	3.00	43.00
	640.00	179.2	0.00	0.28	1623.00	0.00	3.00	44.00
	588.00	232.00	84.00	0.23	989.00	168.00	7.00	77.00

This is a preprint draft. The published article can be found at: https://doi.org/10.1016/j.istruc.2023.07.040.

Please cite this paper as:
Ghasemi A., Naser M.Z., (2023). “Tailoring 3D printed concrete through explainable artificial intelligence.” *Structures*. https://doi.org/10.1016/j.istruc.2023.07.040.

	588.00	232.00	84.00	0.19	1233.00	168.00	7.00	90.00
	840.00	232.00	0.00	0.21	1047.00	0.00	7.00	68.00
	840.00	232.00	0.00	0.05	1304.00	0.00	7.00	77.00
	448.00	179.2	64.00	0.34	1258.00	128.00	7.00	58.00
	448.00	179.2	64.00	0.40	1568.00	128.00	7.00	56.00
	640.00	179.2	0.00	0.32	1302.00	0.00	7.00	55.00
	640.00	179.2	0.00	0.28	1623.00	0.00	7.00	53.00
	588.00	232.00	84.00	0.23	989.00	168.00	28.00	100.00
	588.00	232.00	84.00	0.19	1233.00	168.00	28.00	101.00
	840.00	232.00	0.00	0.21	1047.00	0.00	28.00	95.00
	840.00	232.00	0.00	0.05	1304.00	0.00	28.00	93.00
	448.00	179.2	64.00	0.34	1258.00	128.00	28.00	79.00
	448.00	179.2	64.00	0.40	1568.00	128.00	28.00	72.00
	640.00	179.2	0.00	0.32	1302.00	0.00	28.00	62.00
	640.00	179.2	0.00	0.28	1623.00	0.00	28.00	58.00
Yu, et al. [133]	309.00	321.00	345.00	0.17	345.00	1026.00	1.00	15.00
	309.00	321.00	345.00	0.17	345.00	1026.00	3.00	22.00
	309.00	321.00	345.00	0.17	345.00	1026.00	7.00	28.00
	309.00	321.00	345.00	0.17	345.00	1026.00	28.00	31.00
Pham, et al. [134]	483.00	182.00	268.00	0	1074.00	0	28.00	88.00
Federowicz, et al. [135]	580.00	200.00	83.00	2.17	1234.00	166.00	1.00	35.14
	580.00	189.00	83.00	2.17	1234.00	166.00	1.00	27.70
	580.00	177.00	83.00	2.17	1234.00	166.00	1.00	23.59
	580.00	200.00	83.00	2.17	1234.00	166.00	7.00	71.81
	580.00	189.00	83.00	2.17	1234.00	166.00	7.00	68.02
	580.00	177.00	83.00	2.17	1234.00	166.00	7.00	59.64
	580.00	200.00	83.00	2.17	1234.00	166.00	14.00	79.47
	580.00	189.00	83.00	2.17	1234.00	166.00	14.00	77.29
	580.00	177.00	83.00	2.17	1234.00	166.00	14.00	72.60
	580.00	200.00	83.00	2.17	1234.00	166.00	221.00	81.36
	580.00	189.00	83.00	2.17	1234.00	166.00	21.00	84.06
	580.00	177.00	83.00	2.17	1234.00	166.00	21.00	79.06
	580.00	200.00	83.00	2.17	1234.00	166.00	28.00	84.61
	580.00	189.00	83.00	2.17	1234.00	166.00	28.00	88.23
	580.00	177.00	83.00	2.17	1234.00	166.00	28.00	84.90
Chi, et al. [136]	400.00	168.00	212.00	0.16	80.00	58.80	28.00	18.50

Appendix B

The coding script will be provided upon the publication of this paper.